Quaternary Geochronology 27 (2015) 131–144

Contents lists available at ScienceDirect

Quaternary Geochronology

journal homepage: www.elsevier.com/locate/quageo

Research paper

# Sediment accumulation rates in subarctic lakes: Insights into age-depth modeling from 22 dated lake records from the Northwest Territories, Canada

Carley A. Crann [a, *], R. Timothy Patterson [a], Andrew L. Macumber [a], Jennifer M. Galloway [b], Helen M. Roe [c], Maarten Blaauw [c], Graeme T. Swindles [d], Hendrik Falck [e]

[a] Department of Earth Sciences and Ottawa-Carleton Geoscience Centre, Carleton University, Ottawa, Ontario, K1S 5B6, Canada
[b] Geological Survey of Canada Calgary/Commission Géologique du Canada, Calgary, Alberta, T2L 2A7, Canada
[c] School of Geography, Archaeology and Palaeoecology, Queen's University, Belfast, Belfast, Northern Ireland, BT7 1NN, United Kingdom
[d] School of Geography, University of Leeds, Leeds, LS2 9JT, United Kingdom
[e] Northwest Territories Geoscience Office, Yellowknife, Northwest Territories, X1A 2R3, Canada

ARTICLE INFO

*Article history:*
Received 14 May 2014
Received in revised form
3 February 2015
Accepted 4 February 2015
Available online 7 February 2015

*Keywords:*
Bayesian age-depth modeling
Accumulation rate
Deposition time
Bacon
Subarctic
Northwest Territories
Paleolimnology

ABSTRACT

Age-depth modeling using Bayesian statistics requires well-informed prior information about the behavior of sediment accumulation. Here we present average sediment accumulation rates (represented as deposition times, DT, in yr/cm) for lakes in an Arctic setting, and we examine the variability across space (intra- and inter-lake) and time (late Holocene). The dataset includes over 100 radiocarbon dates, primarily on bulk sediment, from 22 sediment cores obtained from 18 lakes spanning the boreal to tundra ecotone gradients in subarctic Canada. There are four to twenty-five radiocarbon dates per core, depending on the length and character of the sediment records. Deposition times were calculated at 100-year intervals from age-depth models constructed using the 'classical' age-depth modeling software Clam. Lakes in boreal settings have the most rapid accumulation (mean DT 20 ± 10 yr/cm), whereas lakes in tundra settings accumulate at moderate (mean DT 70 ± 10 yr/cm) to very slow rates, (>100 yr/cm). Many of the age-depth models demonstrate fluctuations in accumulation that coincide with lake evolution and post-glacial climate change. Ten of our sediment cores yielded sediments as old as c. 9000 cal BP (BP = years before AD 1950). From between c. 9000 cal BP and c. 6000 cal BP, sediment accumulation was relatively rapid (DT of 20–60 yr/cm). Accumulation slowed between c. 5500 and c. 4000 cal BP as vegetation expanded northward in response to warming. A short period of rapid accumulation occurred near 1200 cal BP at three lakes. Our research will help inform priors in Bayesian age modeling.


## 1. Introduction

Lake sediment accumulation rates vary across space and time (Lehman, 1975; Terasmaa, 2011). Characterization of the spatial trends in accumulation rate for a region and within a lake basin is valuable for sample site selection in paleolimnological studies, as it is often favorable to sample lakes with sufficiently high accumulation rates to achieve a desirable temporal resolution in the data. Understanding the temporal variability and timing of major shifts in accumulation rate as well as the causes of major accumulation rate shifts for a region can be extremely valuable for deciding on levels in an age-depth model that would benefit from additional radiocarbon dates. Such changes in accumulation rate can be used to better understand the limnological system of study and the impact of climate change on that system. Moreover, there are many examples where changes in sediment accumulation rate have been linked to climatic change. For example, in the Cathedral Mountains of British Columbia, the highest Holocene levels of sediment yield are coincident with late Holocene (~4000 BP) climate cooling, reduced catchment vegetation and increased terrestrial erosion (Evans and Slaymaker, 2004). Similarly, in a crater lake in equatorial East Africa, Blaauw et al. (2011) found that cooler climate conditions also resulted in reduced vegetation cover and increased

* Corresponding author. Now: Department of Earth Sciences, University of Ottawa, Ottawa, Ontario, K1N 6N5, Canada.
*E-mail addresses:* ccrann@uottawa.ca (C.A. Crann), Tim.Patterson@carleton.ca (R.T. Patterson), andrewmacumber@cmail.carleton.ca (A.L. Macumber), jennifer.galloway@nrcan-rncan.gc.ca (J.M. Galloway), h.roe@qub.ac.uk (H.M. Roe), maarten.blaauw@qub.ac.uk (M. Blaauw), g.t.swindles@leeds.ac.uk (G.T. Swindles), hendrik_falck@gov.nt.ca (H. Falck).

http://dx.doi.org/10.1016/j.quageo.2015.02.001
1871-1014/

terrestrial erosion and allochtonous sediment input into the lake. Knowledge of accumulation rate is also necessary for proxy-based reconstructions of mean fire return interval, rates of vegetation change (Koff et al., 2000; Marlon et al., 2006), and carbon accumulation rate studies (e.g. Charman et al., 2013), for example, that are only as good as the chronologies they are based upon.

The integration of sediment accumulation rate information into Bayesian age-depth models as prior knowledge, or "priors" is particularly important for sections of an age-depth model where the behavior of the model is uncertain (e.g. sparse data, age reversals, age offsets, dates within a radiocarbon plateau). It can be a challenge, however, to estimate the accumulation rate prior. Goring et al. (2012) provided a summary of sediment accumulation rates from 152 lacustrine sites in the northeastern US/southeastern Canada region and found that, in general, sediment accumulated with a DT of around 20 yr/cm. This result is fairly similar to the previous findings of Webb and Webb (1988; 10 yr/cm) for the same region. However, these estimates are too rapid for subarctic and arctic lakes, where a short ice-free season and low availability of organic material relative to more southern sites lead to slow annual sediment accumulation rates (e.g. Saulnier-Talbot et al., 2009).

This paper expands upon the temperate lake research of Goring et al. (2012) and Webb and Webb (1988). We examine Holocene accumulation rate data for 22 lacustrine sites from a latitudinal gradient spanning boreal forest, treeline, and tundra settings in the Northwest Territories, Canada. While this is a much smaller dataset than Webb and Webb (1988) and Goring et al. (2012), it is significant given that it is logistically difficult to obtain sediment records in arctic and subarctic regions due to the lack of infrastructure. Goring et al. (2012) suggest that such regional datasets can provide important prior knowledge to inform Bayesian (and other) age models.

The age-depth models presented in this paper were constructed in support of an interdisciplinary project aimed at better understanding the natural variability of climate along the routed of the Tibbitt to Contowyto Winter Road (TCWR) in the central Northwest Territories (Canada). Increased precision of age-depth models and increased sampling resolution of proxy data from lake sediment cores have permitted higher resolution characterization paleoclimate patterns (e.g. Galloway et al., 2010; Macumber et al., 2012; Upiter et al., 2014).

## 2. Regional setting

Lakes investigated in this study are located in the central Northwest Territories (Fig. 1) in an area underlain by a portion of the Canadian Shield known as the Slave Craton. This section of Archean crust is characterized by a depositional and volcanic history that has been overprinted by multiple phases of deformation and intruded by granitoid plutons (Bleeker, 2002). Major rock units include basement gneisses and metavolcanics, metasedimentary rocks, and widespread gneissic–granitoid plutons (Padgham and Fyson, 1992; Helmstaedt, 2009). This bedrock geology lacks carbon-rich rocks such as limestones or marl, and is unlikely to be a source of '$^{14}$C dead' carbon, which can cause radiocarbon dates to appear anomalously old.

The Slave Craton has been isostatically uplifting since the retreat of the Laurentide Glacier about 10,000–9000 years ago (Dyke and Prest, 1987; Dyke et al., 2003). Glacial-erosional processes have shaped the terrain, which is characterized by a gentle relief of only a few tens of meters (Rampton, 2000). Where bedrock is not exposed, it lies beneath deposits of till and glaciofluvial sediment of varying thickness. The action of glacial erosion and subglacial meltwater

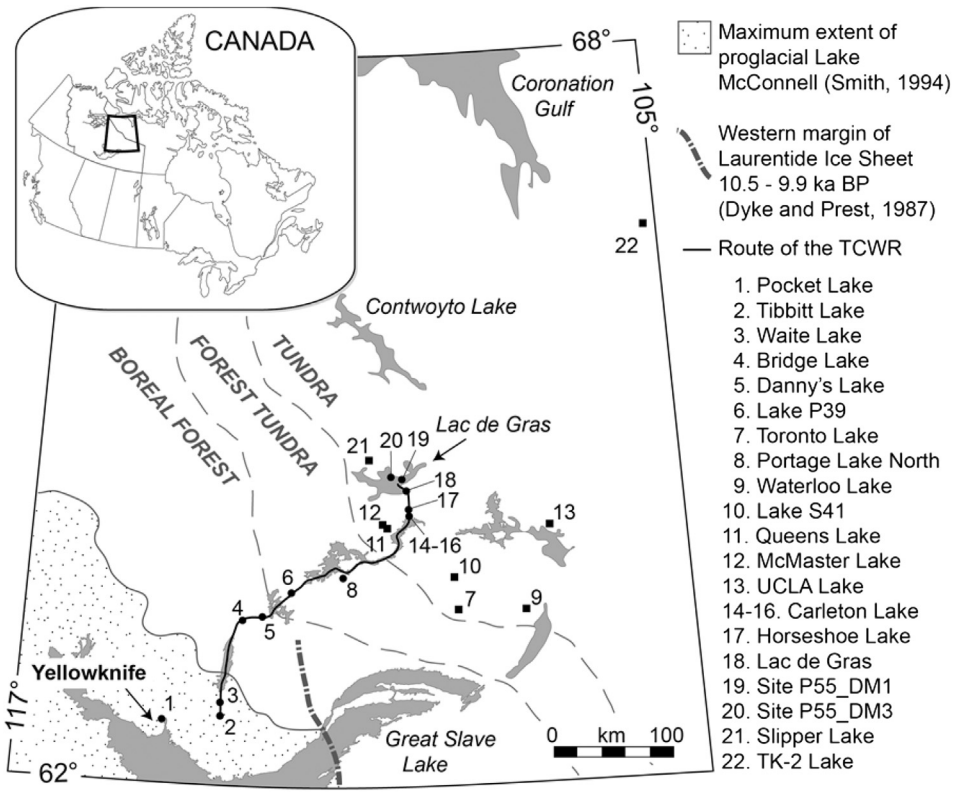


**Fig. 1.** Map of the Northwest Territories showing the locations of core sites. Circles are sites from the TCWR project, squares are sites from previously published work, dashed lines show current boundaries between tundra, forest tundra, and boreal forest ecozones, and the inset shows the location of the study area within Canada. References for the previously published sites are given in Table 1.

flow has resulted in a landscape with abundant, often interconnected lakes. Fig. 1 shows the approximate western margin of the Laurentide Ice Sheet as it retreated toward the east, sometime between 10,500 and 9900 years ago (Dyke and Prest, 1987) as well as the maximum extent of proglacial Lake McConnell (Smith, 1994). Lake McConnell was the main proglacial lake in the region following the retreat of the Laurentide Ice Sheet.

The present-day treeline runs NW/SE across the study area, roughly reflecting the polar front (Fig. 1). The treeline is marked by the northern limits of the boreal forest (Fig. 2A), where forest stands are open and lichen woodlands merge into areas of shrub tundra (Galloway et al., 2010, Fig. 2B). Soils are poorly developed with discontinuous permafrost south of the treeline, and continuous permafrost north of the treeline (Clayton et al., 1977). Tundra vegetation is composed of lichens, mosses, sedges, grasses, and diverse herbs (MacDonald et al., 2009). The vegetation cover and soils are often affected by polygonal permafrost features (Fig. 2C), and are discontinuous on rocky substrates.

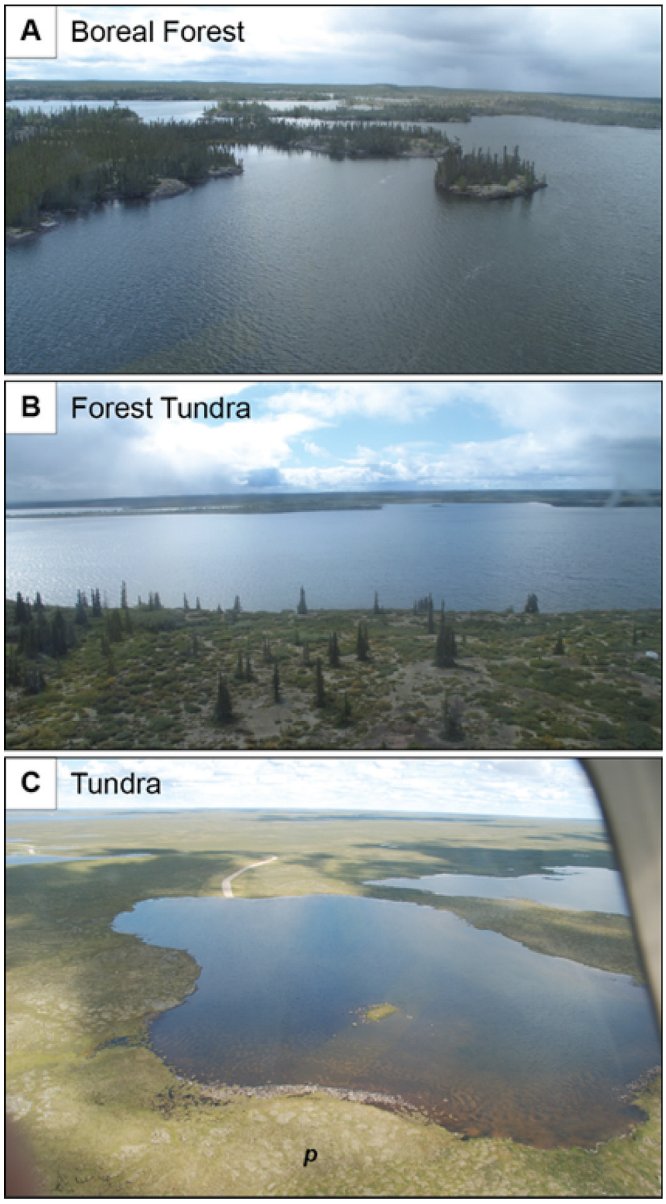


**Fig. 2.** Images of the (A) boreal forest zone at Waite Lake, (B) forest tundra ecotone near Portage Lake North (actually Mackay Lake, not mentioned in this paper), and (C) tundra zone at Carleton Lake, where "p" shows an area with soil polygon development. At Carleton Lake, the path of the TCWR can be seen exiting the lake to the north.

The climate of the region is subarctic continental, characterized by short summers and long cold winters. Annual precipitation is low (175–200 mm) and mean daily January temperatures range from −17.5 °C to −27.5 °C, while mean daily July temperatures range from 7.5 °C to 17.5 °C. Lakes in the region are often ice-covered for much of the year, with an average open-water period of only 90 days (Wedel et al., 1990).

Broad-scale patterns of Holocene climate change in the study area have been identified by proxy evidence from lake sediment cores from Toronto Lake (MacDonald et al., 1993; Wolfe et al., 1996; Pienitz et al., 1999), Waterloo Lake (MacDonald et al., 1993), Lake S41 (MacDonald et al., 2009), Queen's Lake (Moser and MacDonald, 1990; MacDonald et al., 1993; Wolfe et al., 1996; Pienitz et al., 1999), McMaster Lake (Moser and MacDonald, 1990; MacDonald et al., 1993), UCLA Lake (Huang et al., 2004), Slipper Lake (Rühland and Smol, 2005), and Lake TK-2 (Paul et al., 2010) (Fig. 1; Table 1). Based on this body of previous work, three main stages of landscape development have been inferred: (1) between deglaciation (c. 9000 cal BP) and c. 6000 cal BP, terrestrial erosion decreased as vegetation developed from tundra to *Betula*-dominated shrub tundra, and finally to spruce forest tundra (Huang et al., 2004; Sulphur et al., in prep) and stabilized the landscape; (2) between c. 6000 and c. 3500 cal BP the treeline moved north of its present location in response to climate warming (Moser and MacDonald, 1990; MacDonald et al., 1993), likely reflecting a northward retreat of the polar front following the demise of the ice sheet in the middle Holocene (Huang et al., 2004); and (3) between c. 3000 cal BP to the present, there was a general trend towards climate cooling. This resulted in an increase in birch-dominated shrub tundra in the more northerly sites (UCLA lake; Huang et al., 2004). At the more southern locations, vegetation shifts associated with climate change during the latest Holocene are also documented

**Table 1**
Coordinates and physical characteristics of the lakes used in this study.

| Site ID | Site name | TCWR JV[a] ID | Latitude | Longitude | Surface area (ha) | Depth (m) | Citation |
|---|---|---|---|---|---|---|---|
| 1 | Pocket Lake | – | 62°30.540 | 114°22.314 | 6 | 3.5 | |
| 2 | Tibbitt Lake | P0 | 62°32.800 | 113°21.530 | 300 | 6.72 | 10, 11 |
| 3 | Waite Lake | P14-2 | 62°50.987 | 113°19.643 | 100 | 1.8 | 10, 11 |
| 4 | Bridge Lake | P26 | 63°23.297 | 112°51.768 | 119.5 | 4.5 | 11 |
| 5 | Danny's Lake | P34 | 63°28.547 | 112°32.250 | 4.4 | 4.4 | 11 |
| 6 | Lake P39 | P39 | 63°35.105 | 112°18.436 | 37.3 | 1.1 | 11 |
| 7 | Toronto Lake | – | 63°25.800 | 109°12.600 | 10 | 6.75 | 2, 4, 5 |
| 8 | Portage Lake N | P47 | 63°44.538 | 111°12.957 | 194.9 | 4.85 | 11 |
| 9 | Waterloo Lake | – | 63°26.400 | 108°03.600 | ? | ? | 2 |
| 10 | Lake S41 | – | 63°43.110 | 109°19.070 | <0.3 | 4.4 | 8 |
| 11 | Queens Lake | – | 64°07.000 | 110°34.000 | 50 | 4.5 | 1–5 |
| 12 | McMaster Lake | – | 64°08.000 | 110°35.000 | 12 | 8.0? | 1, 2 |
| 13 | UCLA Lake | – | 64°09.000 | 107°49.000 | 28 | 7.7 | 6 |
| 14 | Carleton-1A | P49 | 64°15.571 | 110°05.878 | 29.8 | 15 | 11 |
| 15 | Carleton-1B | P49 | 64°15.571 | 110°05.878 | 29.8 | 1.5 | 11, 12 |
| 16 | Carleton-2012 | P49 | 64°15.500 | 110°05.928 | 29.8 | 3.0 | |
| 17 | Horseshoe Lake | P52 | 64°17.381 | 110°03.701 | 505 | 4.0 | 11 |
| 18 | Lac de Gras | P55 | 64°25.794 | 110°08.168 | ~57 k | 4.0 | 11 |
| 19 | Lac de Gras_DM1 | P55 | 64°30.393 | 110°15.255 | ~57 k | ? | |
| 20 | Lac de Gras_DM3 | P55 | 64°33.723 | 110°26.841 | ~57 k | ? | |
| 21 | Slipper Lake | – | 64°37.000 | 110°50.000 | 190 | 14.0 | 7 |
| 22 | Lake TK-2 | – | 66°20.900 | 104°56.750 | 2.8 | 7.5? | 9 |

Citations: (1) Moser and MacDonald, 1990; (2) MacDonald et al., 1993; (3) Edwards et al., 1996; (4) Wolfe et al., 1996; (5) Pienitz et al., 1999; (6) Huang et al., 2004; (7) Rühland and Smol, 2005; (8) MacDonald et al., 2009; (9) Paul et al., 2010; (10) Galloway et al., 2010; (11) Macumber et al., 2012; (12) Upiter et al., 2014.

[a] TCWR JV = Tibbitt to Contwoyto Winter Road Joint Venture.

(change c. 1000 cal BP at Danny's Lake; Sulphur et al., in prep.).

## 3. Materials and methods

### 3.1. Core collection

The coordinates of each lake, as well as basic lake parameters (surface area, core depth, inlets/outlets) for each site and the relevant references are summarized in Table 1. Data from eight previously published paleolimnological studies located in the area have been incorporated into the dataset to improve perspective on regional trends. The sediment cores from these studies were collected using a modified Livingstone corer (Wright et al., 1984), except the Slipper Lake core, which was collected using a modified KB gravity corer and a mini-Glew gravity corer (Glew, 1991; Glew et al., 2001).

Sampling sites were distributed across the boreal forest, forest-tundra, and tundra ecozones. Coring typically took place during the winter when equipment could be set up directly on the TCWR, thus limiting sites to lakes with winter road access. Water depth was measured in the field using a fish finder (echo sounder). For five lakes, detailed bathymetric profiles were provided by EBA Engineering Consultants Ltd. These profiles were collected during a through-ice bathymetry survey using ground-penetrating radar (GPR) towed behind a vehicle.

The 14 new cores were collected using 1.5–2.0 m long, 10–20 cm wide, freeze corers (hollow, metal-faced corers filled with dry ice; Galloway et al., 2010; Macumber et al., 2012). Freeze corers are ideal for the extraction of cores in unconsolidated and water-saturated sediment as they capture sediment by *in situ* freezing (Lotter et al., 1997; Glew et al., 2001; Kulbe and Niederreiter, 2003; Blass et al., 2007). In 2009, Tibbitt and Waite lakes were cored using a single-sided freeze corer (Galloway et al., 2010). The uppermost sediments from the Waite Lake coring site were unfortunately not recovered as the freeze corer over-penetrated the sediment–water interface during sampling. A Glew core (Glew, 1991) was collected in 2011 in an attempt to capture the missing sediment–water interface. In 2010 a custom designed double-sided freeze corer was deployed in addition to the single-faced corer, to increase the volume of sediment obtained at a given site (Macumber et al., 2012). Freeze cores were sliced at millimeter-scale resolution using a custom designed sledge microtome (Macumber et al., 2011). The highest sampling resolution previously reported previously reported for the region had been half-centimeter intervals from the Slipper Lake (Rühland and Smol, 2005) and Lake S41 cores (MacDonald et al., 2009).

### 3.2. Chronology

With the exception of one twig date in each of the Waite Lake and Queen's Lake cores, and four twig dates in the Lake TK-2 core, radiocarbon dates were obtained from bulk sediment samples, as macrofossils were not encountered during screening. Samples were pretreated with a standard acid wash to remove carbonate material, and unless otherwise stated in Section 4, analyses were performed using the accelerator mass spectrometer (AMS) at the $^{14}$Chrono Dating Laboratory at Queen's University Belfast. Radiocarbon dates reported from previous work employed both conventional and AMS techniques. All radiocarbon ages in were calibrated using either Clam (Blaauw, 2010) or Calib software version 6.1.0 (Stuiver and Reimer, 1993); both programs used the IntCal09 calibration curve (Reimer et al., 2009). Radiocarbon ages younger than AD1950 were calibrated in CALIBomb (Reimer et al., 2004) with the NH_zone1.14c dataset (Hua and Barbetti, 2004). For the Holocene dates used in this study, the differences between the IntCal09 and IntCal13 (Reimer et al., 2013) calibration curves, as well as between the 2004 and 2013 (Hua et al., 2013) postbomb curves are negligible (for our purposes), but we would recommend using the newest curves in future studies. Dates from a $^{210}$Pb profile from Slipper Lake were also incorporated into the dataset (Rühland and Smol, 2005). The Pocket Lake core contains a visible tephra layer, which was geochemically confirmed to as part of the White River Ash deposit (Crann et al., in prep). This horizon will be used in future studies to further constrain the age-depth model. The core from nearby Bridge Lake was analyzed for both visible and cryptotephra, but was unsuccessful in finding evidence for deposition of the White River Ash.

### 3.3. Classical age-depth modeling with Clam

Smooth spline age-depth models were constructed for sediment cores obtained from the TCWR and previously published studies using the 'classical' age-depth modeling software Clam (Blaauw, 2010; R statistical software package) and the IntCal09 calibration curve (Reimer et al., 2009). The year the core was collected was added as the age of the sediment–water interface with an error of ±5 years. The smoothing parameter, which controls how sharply the model will curve toward radiocarbon dates, was increased from the default value of 0.3 to 0.7 for the Danny's Lake model and to 0.5 for the Waite Lake model in order to increase smoothness of the models through the large number of radiocarbon dates. Otherwise, Clam's default smoothing parameter of 0.3 was employed. The core from Lake P39 had only three non-outlying (see next paragraph) dated horizons so the model was constructed using a linear regression. For Slipper Lake, the three uppermost non-interpolated $^{210}$Pb dates were included in the model.

For cores with low dating resolution (typically less than five radiocarbon dates or less than one radiocarbon date per thousand years), suspected outliers were removed on an ad hoc basis when a radiocarbon date either created a clear age reversal in the model or an anomalous shift in accumulation rate that could not be supported by sedimentological evidence (visible color change from gray clay to dark green–brown sediment). We also took into account the regional trends in sediment accumulation rate to aid with outlier identification. For example, many age-depth models show a pronounced decrease in accumulation rate after about 6000 or 5000 cal BP.

The Danny's Lake core is 115 cm long and has a few age reversals among the 25-radiocarbon dates. A Bayesian outlier analysis was performed using the general outlier model (Bronk Ramsey, 2009a) on a sequence in OxCal version 4.1 (Bronk Ramsey, 2009b). This model assumes that the dates are ordered chronologically (dates further down having older ages) and that outliers are in the calendar time dimension and distributed according to a Student-*t* distribution with 5 degrees of freedom (Christen, 1994; Bronk Ramsey, 2009a). Each radiocarbon date was assigned a 5% prior probability of being an outlier. The first outlier analysis identified all three dates at the bottom of the core as outliers so we increased the prior probability of UBA-16439 to 10%, as this date created the largest age reversal. A subsequent outlier analysis still identified the two bottommost dates as outliers and it was unclear as to which was more likely to be an outlier. We then examined the age-depth models from other lakes and from previous studies for clues to resolve this problem. As many of the other models support a higher accumulation rate prior to about 6000 cal BP we used this information to increase the prior probability of UBA-17932 being an outlier to 10%. In Section 5, we show how the Bayesian software Bacon produces age models without performing a separate, formal outlier analysis.

### 3.4. Estimation of deposition time (DT)

An estimate of DT (yr/cm, inverse of accumulation rate) is required as *a priori* information to generate age-depth models

**Table 2**
Radiocarbon ages from all sites, calibrated with the IntCal09 calibration curve (Reimer et al., 2009) using either Calib software version 6.1.0 (Stuiver and Reimer, 1993) or Clam (Blaauw, 2010). The radiocarbon ages younger than AD1950 (italics) were calibrated in CALIBomb (Reimer et al., 2004) with the NH_zone 1.14c dataset (Hua and Barbetti, 2004). The year the core was collected is included as it was used to model the age of the sediment–water interface in the Clam age-depth models. Dates identified as outliers are shown in bold.

| Lake information | Lab ID | Method | Depth (cm) | $^{14}$C age (BP) ± 1σ | Material dated | Cal BP ± 2σ |
|---|---|---|---|---|---|---|
| Pocket Lake collected in 2012 *Freeze core (2F_F1)* | UBA-20676 | AMS | 10–10.5 | 362 ± 27 | Bulk | 310–414 |
| | UBA-22350 | AMS | 20–20.5 | 731 ± 31 | Bulk | 653–727 |
| | UBA-20679 | AMS | 52–52.5 | 1335 ± 25 | Bulk | 1286–1383 |
| | UBA-22351 | AMS | 57–57.5 | 1394 ± 30 | Bulk | 1279–1348 |
| | UBA-22352 | AMS | 70–70.5 | 1725 ± 31 | Bulk | 1556–1708 |
| | UBA-20677 | AMS | 90–90.5 | 2501 ± 30 | Bulk | 2443–2559 |
| | **UBA-22353** | **AMS** | **110–110.5** | **1516 ± 35** | **Bulk** | **1333–1518** |
| | UBA-20678 | AMS | 128.5–129 | 2966 ± 26 | Bulk | 2916–3016 |
| Tibbitt Lake (P0) collected in 2009 *Freeze core (1FR)* | UBA-17353 | AMS | 20–21 | 67 ± 22 | Bulk | (-4)–255 |
| | UBA-17354 | AMS | 40–41 | 1409 ± 20 | Bulk | 1292–1343 |
| | UBA-17355 | AMS | 80–81 | 2046 ± 26 | Bulk | 1930–2111 |
| | Beta-257687 | AMS | 138–138.5 | 2390 ± 40 | Bulk | 2338–2696 |
| Waite Lake (P14-2) collected in 2010 *Glew core* | *UBA-18968* | *AMS* | *17–17.5* | *1.0562 ± 0.003* | *Bulk* | *AD1956–1957* |
| | UBA-18969 | AMS | 27–27.5 | 309 ± 22 | Bulk | 304–455 |
| | UBA-18970 | AMS | 37–37.5 | 556 ± 26 | Bulk | 522–637 |
| Waite Lake (P14-2) collected in 2009 *Freeze core (1FR)* | UBA-18474 | AMS | 0 | 1084 ± 41 | Bulk | 927–1066 |
| | UBA-16433 | AMS | 16.9 | 995 ± 24 | Bulk | 800–961 |
| | UBA-16434 | AMS | 29.1 | 1129 ± 22 | Bulk | 965–1076 |
| | UBA-16435 | AMS | 43.2 | 1455 ± 23 | Bulk | 1304–1384 |
| | UBA-16436 | AMS | 57.8 | 1519 ± 22 | Bulk | 1345–1514 |
| | Beta-257686 | AMS | 66.3 | 1520 ± 40 | Bulk | 1333–1520 |
| | UBA-15638 | AMS | 109.7 | 2107 ± 29 | Twig | 1997–2149 |
| | Beta-257688 | AMS | 154 | 2580 ± 40 | Bulk | 2498–2769 |
| | Beta-257689 | AMS | 185 | 2920 ± 40 | Bulk | 2955–3210 |
| | Beta-257690 | AMS | 205.1 | 3460 ± 40 | Bulk | 3633–3838 |
| Bridge Lake (P26-1) collected in 2010 *Freeze core (2F_F2)* | UBA-18964 | AMS | 6.5–7 | 28 ± 23 | Bulk | (-4)–244 |
| | UBA-22873 | AMS | 12.5–13 | 694 ± 26 | Bulk | 565–683 |
| | UBA-18965 | AMS | 18–18.5 | 1883 ± 23 | Bulk | 1736–1882 |
| | UBA-22874 | AMS | 24.5–25 | 3782 ± 30 | Bulk | 4082–4246 |
| | UBA-22875 | AMS | 30.5–31 | 4730 ± 30 | Bulk | 5326–5583 |
| | UBA-22876 | AMS | 34.5–35 | 5487 ± 31 | Bulk | 6210–6322 |
| | UBA-18966 | AMS | 41.5–42 | 5816 ± 42 | Bulk | 6501–6727 |
| | UBA-22877 | AMS | 50.5–51 | 6184 ± 32 | Bulk | 6977–7172 |
| | UBA-18967 | AMS | 59.5–60 | 6762 ± 32 | Bulk | 7576–7667 |
| | UBA-22878 | AMS | 64–64.5 | 7025 ± 34 | Bulk | 7788–7941 |
| Danny's Lake (P34-2) collected in 2010 *Freeze core (2F_F2)* | UBA-17359 | AMS | 5.7 | 693 ± 21 | Bulk | 567–679 |
| | UBA-17360 | AMS | 10.2 | 855 ± 23 | Bulk | 695–795 |
| | UBA-16543 | AMS | 15–15.5 | 1329 ± 23 | Bulk | 1184–1299 |
| | UBA-17361 | AMS | 21.9 | 1617 ± 25 | Bulk | 1416–1556 |
| | UBA-17431 | AMS | 27.8 | 1659 ± 21 | Bulk | 1521–1615 |
| | UBA-16544 | AMS | 32.6 | 1916 ± 25 | Bulk | 1818–1904 |
| | UBA-20377 | AMS | 33.5 | 2071 ± 24 | Bulk | 1987–2120 |
| | UBA-20378 | AMS | 34.2 | 2159 ± 24 | Bulk | 2061–2305 |
| | UBA-17929 | AMS | 34.5 | 2257 ± 26 | Bulk | 2158–2343 |
| | **UBA-20376** | **AMS** | **35.3** | **2073 ± 28** | **Bulk** | **1986–2124** |
| | UBA-20375 | AMS | 36.8 | 2248 ± 25 | Bulk | 2158–2339 |
| | **UBA-17432** | **AMS** | **37.6** | **2659 ± 32** | **Bulk** | **2742–2884** |
| | UBA-20374 | AMS | 38.4 | 2392 ± 25 | Bulk | 2345–2488 |
| | UBA-20373 | AMS | 39.3 | 2448 ± 33 | Bulk | 2358–2702 |
| | UBA-17930 | AMS | 40.4 | 2549 ± 26 | Bulk | 2503–2748 |
| | UBA-20371 | AMS | 41.4 | 2554 ± 28 | Bulk | 2503–2750 |
| | **UBA-20372** | **AMS** | **43.3** | **4863 ± 29** | **Bulk** | **5583–5652** |
| | UBA-16545 | AMS | 45–45.5 | 2912 ± 24 | Bulk | 2964–3157 |
| | UBA-16546 | AMS | 56.9 | 3604 ± 25 | Bulk | 3845–3975 |
| | UBA-16547 | AMS | 70.1 | 5039 ± 51 | Bulk | 5661–5903 |
| | UBA-16548 | AMS | 85–85.5 | 5834 ± 29 | Bulk | 6560–6733 |
| | UBA-17931 | AMS | 89.5 | 6231 ± 34 | Bulk | 7016–7253 |
| | **UBA-16439** | **AMS** | **95.5** | **8112 ± 32** | **Bulk** | **8997–9125** |
| | **UBA-17932** | **AMS** | **99.1** | **7623 ± 38** | **Bulk** | **8370–8518** |
| | UBA-16440 | AMS | 113.6 | 7450 ± 30 | Bulk | 8191–8346 |
| P39-1A collected in 2010 *Freeze core (2F_F1)* | **UBA-17344** | **AMS** | **10–10.5** | **3597 ± 26** | **Bulk** | **3840–3973** |
| | UBA-17345 | AMS | 19–19.5 | 3701 ± 24 | Bulk | 3974–4144 |
| | UBA-17346 | AMS | 29–29.5 | 5385 ± 35 | Bulk | 6018–6284 |
| Toronto Lake collected in 1987 *Livingstone core* | Beta-49705 | conv. | 35–50 | 1760 ± 90 | Bulk | 1421–1887 |
| | Beta-53129 | conv. | 80–85 | 4200 ± 80 | Bulk | 4450–4956 |
| | Beta-53130 | conv. | 125–130 | 5460 ± 90 | Bulk | 6001–6408 |
| | Beta-49708 | conv. | 155–160 | 7040 ± 120 | Bulk | 7657–8155 |
| Portage Lake N. (P47-1) collected in 2010 *Freeze core (2F_F2)* | UBA-17933 | AMS | 6.5–7 | 772 ± 24 | Bulk | 673–729 |
| | UBA-17159 | AMS | 13.5–14 | 4218 ± 38 | Bulk | 4626–4854 |
| | **UBA-17160** | **AMS** | **41–41.5** | **4885 ± 37** | **Bulk** | **5584–5710** |

(*continued on next page*)

**Table 2** (*continued*)

| Lake information | Lab ID | Method | Depth (cm) | $^{14}$C age (BP) ± 1σ | Material dated | Cal BP ± 2σ |
|---|---|---|---|---|---|---|
| | UBA-17161 | AMS | 63–63.5 | 5333 ± 35 | Bulk | 5997–6264 |
| | UBA-17162 | AMS | 86.5–87 | 5878 ± 34 | Bulk | 6637–6783 |
| Waterloo Lake collected in 1987? *Livingstone core* | **TO-3312** | **AMS** | **28–31** | **4030 ± 50** | **Bulk** | **4413–4801** |
| | TO-3311 | AMS | 54–56 | 4640 ± 50 | Bulk | 5090–5577 |
| | TO-3310 | AMS | 61–63.5 | 5300 ± 50 | Bulk | 5939–6257 |
| | TO-3313 | AMS | 75–77 | 7640 ± 100 | Moss | 8206–8627 |
| Lake S41 collected in 2005 *Livingstone core* | UCI-25833 | AMS | 7–7.5 | 375 ± 15 | Bulk | 331–499 |
| | UCI-25841 | AMS | 13.4–14 | 1045 ± 20 | Bulk | 926–1042 |
| | UCI-25836 | AMS | 23–23.5 | 1985 ± 15 | Bulk | 1892–1987 |
| | UCI-25835 | AMS | 32.5–33 | 2765 ± 20 | Bulk | 2789–2924 |
| Queen's Lake collected in 1987? *Livingstone core* | WAT-1770 | conv. | 15–20 | 3820 ± 60 | Bulk | 4010–4414 |
| | WAT-1771 | conv. | 45–50 | 5600 ± 60 | Bulk | 6291–6493 |
| | WAT-1772 | conv. | 60–65 | 6150 ± 60 | Bulk | 6888–7241 |
| | WAT-1773 | conv. | 100–105 | 7150 ± 70 | Bulk | 7842–8159 |
| | TO-827 | AMS | 105 | 7470 ± 80 | Twig | 8060–8417 |
| McMaster Lake collected in 1987? *Livingstone core* | **TO-766** | **AMS** | **10–12** | **3690 ± 50** | **Bulk** | **3888–4212** |
| | TO-158 | AMS | 20–22 | 3680 ± 60 | Bulk | 3849–4220 |
| | TO-767 | AMS | 30–32 | 5120 ± 60 | Bulk | 5730–5990 |
| | TO-156 | AMS | 40–42 | 5360 ± 60 | Bulk | 5998–6279 |
| | TO-154 | AMS | 60–62 | 6180 ± 60 | Bulk | 6943–7248 |
| UCLA Lake *Livingstone core* | TO-8840 | AMS | 20–21 | 2370 ± 50 | Bulk | 2319–2698 |
| | TO-8842 | AMS | 35–35.5 | 4130 ± 50 | Bulk | 4527–4824 |
| | TO-8844 | AMS | 45–45.5 | 5680 ± 70 | Bulk | 6317–6635 |
| | TO-8845 | AMS | 50–50.5 | 6280 ± 70 | Bulk | 7002–7413 |
| | TO-8846 | AMS | 55.5–56 | 7040 ± 70 | Bulk | 7707–7978 |
| | TO-8847 | AMS | 64.5–65 | 7680 ± 70 | Bulk | 8382–8590 |
| | TO-8848 | AMS | 69.5–70 | 7960 ± 80 | Bulk | 8605–9006 |
| Carleton Lake (P49-1A) collected in 2010 *Freeze core (2F_F2)* | **UBA-19464** | **AMS** | **9.5–10** | **2794 ± 34** | **Bulk** | **2791–2970** |
| | **UBA-20002** | **AMS** | **15–15.5** | **2778 ± 26** | **Bulk** | **2793–2950** |
| | UBA-20003 | AMS | 25–25.5 | 2716 ± 33 | Bulk | 2757–2868 |
| | UBA-19465 | AMS | 32.5–33 | 3124 ± 41 | Bulk | 3254–3443 |
| | UBA-19466 | AMS | 40.5–41 | 3616 ± 37 | Bulk | 3835–4075 |
| | UBA-19467 | AMS | 66.5–67 | 4927 ± 38 | Bulk | 5594–5728 |
| Carleton Lake (P49–1B) collected in 2010 *Freeze core (1F)* | *UBA-18472* | *AMS* | *0–0.5* | *1.0264 ± 0.0035* | *Bulk* | *AD1955–1957* |
| | UBA-17934 | AMS | 10–10.5 | 1046 ± 24 | Bulk | 925–983 |
| | UBA-17347 | AMS | 19.5–20 | 1925 ± 25 | Bulk | 1822–1926 |
| | UBA-17935 | AMS | 40–40.5 | 2762 ± 35 | Bulk | 2780–2946 |
| | UBA-17348 | AMS | 64.5–65 | 3675 ± 24 | Bulk | 3926–4087 |
| | UBA-17936 | AMS | 80–80.5 | 4635 ± 32 | Bulk | 5304–5465 |
| | UBA-17349 | AMS | 100–100.5 | 5663 ± 26 | Bulk | 6399–6497 |
| Carleton Lake (R12-P49) collected in 2012 *Freeze core (2F_F2)* | UBA-20612 | AMS | 10.0 | 702 ± 39 | Bulk | 560–699 |
| | UBA-20613 | AMS | 36.2 | 1337 ± 31 | Bulk | 1181–1305 |
| | UBA-20614 | AMS | 55.3 | 1302 ± 46 | Bulk | 1132–1304 |
| | UBA-20615 | AMS | 81.5 | 2132 ± 31 | Bulk | 2002–2299 |
| | UBA-20616 | AMS | 117.8 | 2944 ± 32 | Bulk | 2989–3216 |
| Horseshoe Lake (P52-1) collected in 2010 *Freeze core (2F_F2)* | UBA-17350 | AMS | 9–9.5 | 178 ± 25 | Bulk | (-2)–291 |
| | UBA-17163 | AMS | 18–18.5 | 1148 ± 42 | Bulk | 967–1172 |
| | UBA-17351 | AMS | 28–28.5 | 2763 ± 22 | Bulk | 2785–2924 |
| | UBA-17352 | AMS | 38–38.5 | 3343 ± 23 | Bulk | 3481–3639 |
| | UBA-19973 | AMS | 43.2 | 3776 ± 36 | Bulk | 3992–4281 |
| | UBA-17938 | AMS | 46–46.5 | 4885 ± 27 | Bulk | 5589–5653 |
| | UBA-17165 | AMS | 55–55.5 | 5916 ± 58 | Bulk | 6628–6897 |
| | UBA-17937 | AMS | 68–68.5 | 6723 ± 29 | Bulk | 7516–7656 |
| | UBA-17166 | AMS | 80–80.5 | 7488 ± 40 | Bulk | 8199–8383 |
| | UBA-17167 | AMS | 106–106.5 | 8011 ± 43 | Bulk | 8718–9014 |
| Lac de Gras (LDG) collected in 2010 *Freeze core (2F_F2)* | UBA-17939 | AMS | 12–12.5 | 1123 ± 23 | Bulk | 965–1067 |
| | **UBA-17356** | **AMS** | **19–19.5** | **3299 ± 38** | **Bulk** | **3447–3631** |
| | UBA-17357 | AMS | 32–32.5 | 1607 ± 29 | Bulk | 1412–1551 |
| | UBA-17358 | AMS | 46–46.5 | 2144 ± 35 | Bulk | 2003–2305 |
| Lac de Gras (LDG_DM1) collected in 2012 *Freeze core* | D-AMS 001550 | AMS | 10–11 | 784 ± 23 | Bulk | 677–732 |
| | D-AMS 001551 | AMS | 20–21 | 1797 ± 23 | Bulk | 1629–1817 |
| | D-AMS 001552 | AMS | 30–31 | 2636 ± 25 | Bulk | 2738–2781 |
| | D-AMS 001553 | AMS | 40–41 | 3590 ± 27 | Bulk | 3836–3972 |
| Lac de Gras (LDG_DM3) collected in 2012 *Freeze core* | D-AMS 001554 | AMS | 10–11 | 1719 ± 23 | Bulk | 1561–1696 |
| | D-AMS 001555 | AMS | 20–21 | 3459 ± 26 | Bulk | 3642–3828 |
| | D-AMS 001556 | AMS | 30–31 | 5509 ± 28 | Bulk | 6223–6396 |
| | D-AMS 001557 | AMS | 40–41 | 7827 ± 31 | Bulk | 8543–8696 |
| Slipper Lake collected in 1997 *KB gravity and mini-Glew* | $^{210}$PB Age | n/a | 0 | n/a | Bulk | (-49)–(-45) |
| | $^{210}$PB Age | n/a | 2 | n/a | Bulk | 6–20 |
| | $^{210}$PB Age | n/a | 3 | n/a | Bulk | 34–94 |
| | TO-9671 | AMS | 21.5–22.5 | 3270 ± 80 | Bulk | 3359–3688 |
| | TO-9672 | AMS | 43.5–44.5 | 4760 ± 70 | Bulk | 5321–5603 |
| Lake TK-2 collected in 1996 *Livingstone core* | Beta-167871 | AMS | 32–34 | 2480 ± 40 | Bulk | 2365–2718 |
| | Beta-167872 | AMS | 60–62 | 3870 ± 40 | Bulk | 4157–4416 |
| | Beta-167873 | AMS | 96–98 | 5670 ± 40 | Bulk | 6322–6558 |

**Table 2** (*continued*)

| Lake information | Lab ID | Method | Depth (cm) | $^{14}$C age (BP) ± 1σ | Material dated | Cal BP ± 2σ |
|---|---|---|---|---|---|---|
| | TO-7871 | AMS | 132 | 7370 ± 80 | Twigs | 8020–8349 |
| | TO-7870 | AMS | 137 | 7190 ± 80 | Twigs | 7860–8178 |
| | TO-7869 | AMS | 142 | 7740 ± 90 | Twigs | 8375–8772 |
| | TO-7868 | AMS | 174 | 7780 ± 70 | Twigs | 8412–8761 |

using the Bayesian software Bacon (Blaauw and Christen, 2011). This estimate can be based on prior knowledge obtained from previously built age-depth models from lakes in the region (Goring et al., 2012). Here we generate a summary for the region using the age-depth models constructed in Clam to calculate the DT at 100-year intervals for each model. It should be noted that the intention of the summary is to produce initial estimates of DT for age-depth modeling and the data has not undergone a rigorous statistical analysis. The DT between the uppermost non-outlying date and the date used to model the surface age were not included in graphing the accumulation rates because: (1) there is potential uncertainty with the assumption that the age of the sediment–water interface is indeed the year that the core was collected; and (2) high water content in the uppermost sediments can lead to an anomalously rapid DT. Webb and Webb (1988) assumed 50% compaction in sediments below the uppermost 5–10 cm of the sediment column based on dry weight/wet weight ratios, yet they found that the accumulation rates were still higher during the historic period. Because dry weight/wet weight data has not been collected for this study, the effect of compaction and dewatering is not taken into account in graphing the DT. P39 and Slipper lake cores lacked sufficient chronological control and were omitted from the DT compilation dataset.

## 4. Results

The radiocarbon dates from all sites included in this study, along with the results from the outlier analysis, are summarized in Table 2. The age-depth models constructed using Clam have been grouped into three categories (Fig. 3). The first category, rapid sediment accumulation rate lakes, contains five age-depth models that stand out from the rest. Deposition times in this category do not tend to exceed 50 yr/cm, and the average DT (rounded to the nearest 10 = 20 yr/cm) is on par with lakes in the Great Lakes region (Goring et al., 2012). The other two categories, moderate and slow sediment accumulation rate lakes, are not so easily distinguished. Accumulation rates for age-depth models in both categories fluctuate, but moderate sediment-rate accumulating sites tend to fluctuate at more subtle amplitudes (DT of around 50 yr/cm) and do not often exceed a DT of 100 yr/cm. Sites with overall slow accumulation rates fluctuate with DT amplitudes up to 150 yr/cm, and tend to be in excess of 100 yr/cm.

Detailed results for each category are given in Sections 4.1–4.3. Because these results are intended to yield insight into the spatial and temporal variability in accumulation rates in high latitude lakes and to give estimates of DT that can be used as prior information in Bayesian age-depth modeling with Bacon, DTs are rounded to the nearest 10 yr/cm.

### 4.1. Sites with rapid accumulation rates (DT < 50 yr/cm)

Rapid sediment accumulation rates are defined as having the DT for the majority of the core of less than 50 yr/cm. Five distinctive age depth models belonging to this category were produced for cores from Lac de Gras, Pocket, Tibbitt, Waite and Carleton lakes. Due to rapid sediment accumulation rates, these core records tend to span ~3500 years at most. The cores in this category yielded internally consistent age-depth models, with the exception of one radiocarbon date that is a clear outlier in the Lac de Gras core (Table 2). The average DT (rounded to the nearest 10 = 20 yr/cm) is on par with lakes in the Great Lakes region (Goring et al., 2012).

Deposition times in these lakes vary between c. 10 and 50 yr/cm, with a mean of c. 20 ± 10 yr/cm (1σ) and a unimodal distribution, based on 107 DT measurements at 100-year intervals (Fig. 4A). The accumulation pattern for Tibbitt Lake is different from the others as it increases steadily from a DT of c. 5 yr/cm at c. 2500 cal BP to c. 50 yr/cm at the top, but the very rapid deposition near the base overlaps the Hallstatt Plateau (c. 2700–2300 cal BP; Blockley et al., 2007), which is a flat section in the IntCal09 calibration curve and therefore may be an artifact of calibration.

### 4.2. Sites with moderate accumulation rates (DT 50–100 yr/cm)

The distinguishing characteristics of sites within this category include fluctuations in sediment accumulation rate at relatively subtle amplitudes (DT around 50 yr/cm) and DTs that do not generally exceed 100 yr/cm. The sites in this category are Danny's, Toronto, S41, Carleton-1A, Carleton-1B, LDG_DM1, and TK-2. Three of the cores in the moderate accumulation rate category are characterized by a sedimentary record that extends just beyond 8000 cal BP. The other four cores in this category have records that extend back between c. 6000 and c. 4000 cal BP (Fig. 3).

The outlier analysis performed in OxCal identified five outliers in the Danny's Lake core, which were omitted from the smooth spline age-depth model constructed with Clam. Four of the five outliers were older than the model and the fifth was only slightly younger. For Carleton-1A, the upper three radiocarbon dates, at 9.5, 15 and 25 cm, all overlapped within the age range of c. 2900 to c. 2700 cal BP. For this reason the uppermost two dates were omitted from the age-depth model constructed in Clam. The overlap may have been the result of sediment mixing. The core from Lake TK-2 has an age reversal within the bottommost four dates. Because these dates were obtained from twigs (allochthonous origin and lack of heartwood), the reversal is likely due to delayed deposition of older organic material. Clam was able to accept the reversal as the date was within error of the others.

The lakes in this category accumulated with DTs between 50 and 100 yr/cm with a mean of c. 70 ± 20 yr/cm (1σ) based on 343 DT measurements at 100-year intervals (Fig. 4). The histogram shown in Fig. 4A has a bimodal distribution with a primary mode around 60 yr/cm and a secondary mode around 100 yr/cm. Most of the lakes in this category exhibit fluctuations in accumulation rate over time.

### 4.3. Sites with slow accumulation rates (DT 100–250 yr/cm)

Accumulation rates fluctuate in age-depth models for lakes with moderate and slow rates, producing some overlapping characteristics. Sites with overall slow accumulation rates fluctuate with DT amplitudes up to 150 yr/cm that tend to exceed 100 yr/cm. The sites in the slow accumulation category are Bridge, Waterloo, UCLA, Horseshoe, and LDG_DM3. All five sites in this category extend back to at least c. 8000 cal BP or beyond. The age-models are internally

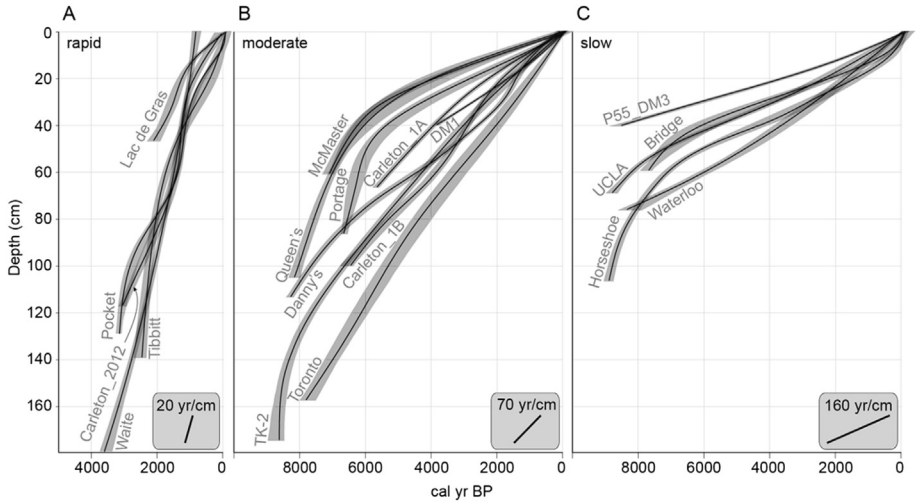


**Fig. 3.** Age-depth models constructed using a smooth spline regression in Clam, grouped into (A) rapid, (B) moderate, and (C) slowly accumulating sites. The 95% confidence interval is light gray. The scale for Waite Lake is to be used as a relative measure only as the freeze corer over-penetrated the sediment–water interface.

consistent, with only one outlier identified from the Waterloo Lake age-depth model, where the age is older than the model (Fig. 3).

The histogram of DTs (Fig. 4A) is multi-modal, reflecting high variability of sediment accumulation rates for cores within this category. The main pattern occurs between about 8000 and 5000 cal BP, where Bridge, UCLA, and Horseshoe lakes are all characterized by a slowing of accumulation rate (increased DT). This rate change is coincident with changes in sedimentation from minerogenic-rich at the base of the core to organic-rich above (Macumber et al., 2012). For Bridge Lake, the accumulation rate slows steadily from a DT of ~50 yr/cm at 7600 cal BP to c. 200 yr/cm at 4000 cal BP. This accumulation rate change is linked to a distinct color change at ~4200 cal BP, from light gray below (Munsell code 5y 3/2) to brown (Munsell code 10 yr 2/1) above (Macumber et al., 2012). The DT is constant around 200 yr/cm until c. 2500 cal BP and steadily changes to c. 160 yr/cm by 100 cal BP.

The accumulation rate profile for Horseshoe Lake displayed the highest variability of any studied profile. Modeled DT is rapid (c. 20 yr/cm) between 8700 and 7500 cal BP and then slows to c. 225 yr/cm by 5000 cal BP. The transition around 7500 cal BP is associated with a shift from minerogenic-rich sediment at the core bottom to organic-rich sediment above. C/N ratios from Horseshoe Lake suggest that the sub-basin of Horseshoe Lake has undergone fluctuations in water depth (Griffith, 2013). Therefore, it is possible that there is a hiatus in deposition between c. 6,000 and c. 4,000 cal BP. A hiatus would also explain the anomalously slow accumulation rates. Stratigraphically above ~7500 cal BP, the accumulation rate gradually increases; DT reaching c. 100 yr/cm by 3000 cal BP, then decreasing to 150 yr/cm by 2000 cal BP, and finally increases again to 60 yr/cm at the core top.

### 4.4. Sites with poor chronological constraint

Some sites do not easily fit into the three recognized categories, either due to lack of dating resolution (P39 and Slipper lakes) or because the accumulation profile is characterized by a dramatic shift in accumulation rate (Portage North, Queens, and McMaster; Fig. 4). P39, Portage North, and McMaster lakes all had one outlier – identified on an ad hoc basis – that fell between 5000 and 4000 cal BP (Fig. 3). For P39, the radiocarbon date at the top of the core was determined to be an outlier. Because the core was collected in only 110 cm water depth, upper lake sediments may have been disturbed due to freezing of ice to the sediment–water interface. No further research was undertaken on this core and accumulation rates were not estimated. Slipper Lake lacked sufficient chronological control (based on two $^{14}$C dates and a $^{210}$Pb profile) and was also omitted from calculations of accumulation rate.

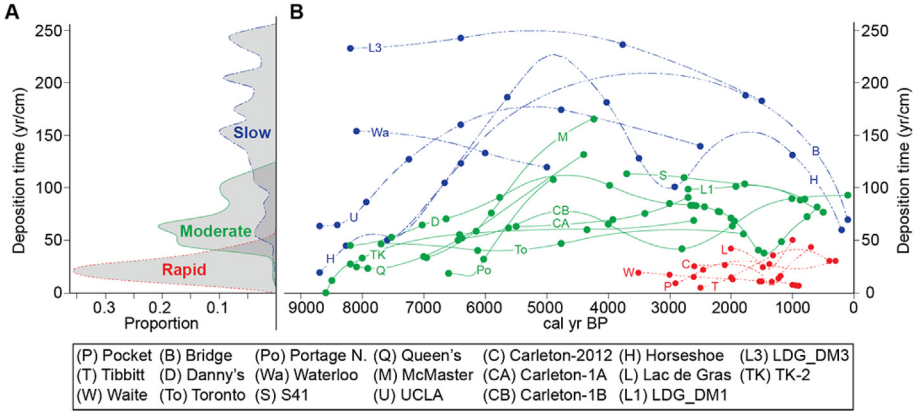


**Fig. 4.** (A) Histogram of DT from rapid, moderate, and slowly accumulating lake site categories, sampled at 100-year intervals from the age-depth models constructed in Clam. (B) Accumulation rate profiles for each site showing fluctuation of DT over time and the variability between lake sites. The dots correspond to radiocarbon dates.

## 5. Bayesian age-depth modeling with Bacon

The temporal and spatial variations identified above are used as prior information for three Bayesian age-depth models to demonstrate the power and robustness of this approach. The age modeling procedure for Bacon is similar to that outlined in Blaauw and Christen (2005), but more numerous and shorter sections are used to generate a more flexible chronology (Blaauw and Christen, 2011, 2013). Radiocarbon age distributions are modeled using the Student-*t* distribution, which produces calibrated distributions with longer tails than obtained using the Normal model (Christen and Pérez, 2009). Due to the longer tails on radiocarbon dates and a prior assumption of unidirectional sediment accumulation, in most cases excluding outliers is not necessary when using Bayesian age modeling. The cores from Waite, Danny's and Horseshoe lakes all have at least ten non-outlying radiocarbon dates and were deemed suitable for Bayesian modeling with Bacon.

As this is a demonstration of the practical application of Bacon (version 2.2; Blaauw and Christen, 2011, 2013), text in italics denotes the actual code typed in R (statistical computing and graphics software). Bacon version 2.2 uses the currently most recent calibration curve, IntCal13 (Reimer et al., 2013), and has an added feature of plotting accumulation rate data with the *plot.accrate.depth()* and *plot.accrate.age()* functions. In Section 6.3 we show a practical example of the accumulation rate plotting function.

Memory or coherence in accumulation rates along the core is a parameter that is defined based on the degree to which the accumulation rate at each interval depends on the previous interval. For example, the memory for modeling accumulation in peat sediments should be higher than for lacustrine sediments because accumulation of peat in peat bogs is less dynamic over time than the accumulation of sediments in a lake. Here we used the memory properties from the lake example in Blaauw and Christen (2011; *mem.strength = 20* and *mem.mean = 0.1*).

The accumulation rates (*acc.rate=*) for Waite and Danny's lakes were based on the DT estimates from Section 4 (20, and 70, respectively). The accumulation shape (*acc.shape=*) for the Waite Lake cores was set to 2, as suggested by Blaauw and Christen (2011). The accumulation shape controls how much influence the accumulation rate will have on the model. The default value of 2 is fairly low, thus the model has a fair amount of freedom to adapt rates to what the data suggest. For the Danny's lake age model, the accumulation shape was increased to a value of 20 to avoid perturbations in the model caused by known outliers. The step size for Waite Lake was set to 5 cm, which is the default for a lake (Blaauw and Christen, 2011). The Danny's lake age-depth model required more flexibility due to the observed shifts in accumulation rate that are unlikely to be the product of spurious radiocarbon ages (they are sustained changes coherent with known climate events), so the step sizes was lowered to 2 cm.

Horseshoe Lake required the addition of a hiatus (*hiatus.depths = 45, hiatus.mean = 10*) in order to produce a realistic, stable model. Because the hiatus accounts for the slowest accumulation rates for the age-depth model (>150 yr/cm between c. 6000–4000 cal BP), the portion of the model below the hiatus accumulates at moderate rate (*acc.mean = 70, acc.shape = 2*) and the portion of the model above the hiatus rate (*acc.mean = 20, acc.shape = 1*). The physical nature of this hiatus is explored in Section 6.2.

The resulting age-depth models are shown in Fig. 5, along with plots that describe: (1) the stability of the model (log objective vs. iteration); (2) the prior (entered by the user) and posterior (resulting) accumulation rate, and; (3) the prior and posterior memory properties. The Bayesian model from Waite Lake shows stable accumulation rates over time, most likely because this core covers the latest Holocene, during which time climate was relatively consistent (Karst-Riddoch et al. 2005; Rühland and Smol, 2005; Miller et al. 2010). Danny's Lake also yielded a stable model, with the consideration that the weight on accumulation rate was set very high. The Horseshoe Lake model ran fairly stable, with a minor perturbation.

The prior and posterior probability diagrams for accumulation rate were fairly similar for Waite and Danny's lakes, and for Horseshoe Lake, the posterior distribution for accumulation rate is a combination of the two assigned rates. Waite and Danny's lakes models both showed memory of around 0.25, which is higher than was assigned (0.1). The Horseshoe Lakes model had far less memory than assigned, but this is because memory falls to 0 across a hiatus.

## 6. Discussion

### 6.1. Spatial variability in accumulation rates

The three southernmost boreal forest lakes (Pocket, Tibbitt, and Waite) have the highest accumulation rates, suggesting that the accumulation rate may be related to in-lake productivity and in-wash of organic detritus. Sediment accumulation rates at Bridge and Danny's lakes are slower than the more productive boreal lakes; Pocket, Tibbitt, and Waite lakes. The last c. 3000 years of accumulation at Danny's lake mirrors the pattern of rapidly accumulating sites, but is slower by a DT of about 10–20 yr/cm. This suggests that Danny's lake responded similarly to climate as the southernmost lakes, but may either be slightly less productive due to colder temperatures at its location closer to the polar front, or, judging by the bathymetry (Fig. 6), the coring site itself may receive less sediment than the main basin of the lake, where sediment accumulation is most commonly the greatest (c.f. Lehman, 1975). The accumulation rate at Bridge Lake is extremely slow for the location south of the treeline and again we look at the bathymetry for an explanation (Fig. 6). The coring location for Bridge Lake is nestled into a steep slope, proximal to a deeper sub-basin with a much thicker sediment package. The slope limits the amount of sediment that can accumulate at this site, and similarly to Danny's Lake, much of the material is likely to have drifted toward the deeper basin.

Two of the most rapidly accumulating lakes are located in the tundra (Carleton-2012 and Lac de Gras). Examination of the bathymetry profiles reveals certain basin features that could explain the rapid accumulation rates (Fig. 6). Carleton Lake has a shallow shelf over 500 m long that has a maximum depth of two meters, a slope covering less than 100 m, and a main basin that is about 500 m long at a depth of about 4 m (Fig. 6). The Carleton-2012 freeze core was collected from a site closer to the slope and shelf than the Carleton-1A and Carleton-1B freeze cores. The shelf, which is situated in two meters water depth, may be susceptible to re-suspension of fine detritus due to surface waves touching bottom generated during windy or stormy conditions. The re-suspended sediments would be transported down into the basin, with the majority being deposited closer to the slope terminus. A similar trend has been noted at two Lakes in Estonia whereby sediments deposited nearshore are thought to have eroded during a regressive period and redeposited elsewhere (Punning et al., 2007a, 2007b; Terasmaa, 2011). Looking at the bathymetry for Lac de Gras, it would be expected that since the coring site is steep, sediment would by-pass and be deposited in the deeper part of the lake. It is unclear, however, if there is a sub-basin at the coring site due to the low resolution of the available bathymetry (Fig. 6). The coring site was characterized by turbid water, steep surrounding landscape, and high minerogenic content of the core sediments (Macumber et al., 2012). Therefore, the rapid accumulation rate at this site is

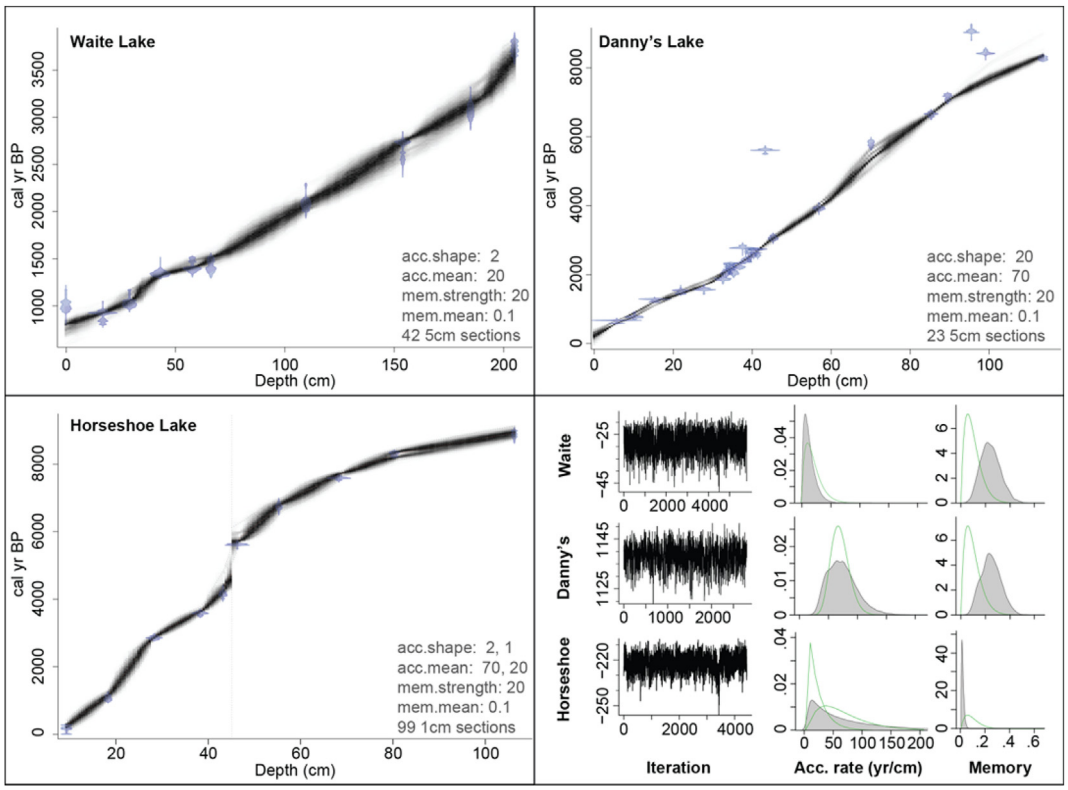


**Fig. 5.** Bayesian age-depth models constructed with the age-depth modeling software Bacon for Waite, Danny's, and Horseshoe lake cores. The grayscale on the model represents the likelihood, where the darker the gray, the more likely the model is of running through that section. The vertical, dashed line on the Horseshoe Lake model denotes a hiatus. The bottom right panel shows three plots for each model: (left) stability of the model; (middle) prior (line) and posterior (filled) distributions of accumulation mean; and (right) prior (line) and posterior (filled) distributions of memory properties.

likely due to in-wash of material from the lake catchment. The other two cores from Lac de Gras (DM1 and DM3) are in a completely different sub-basin of the lake. These cores exhibit moderate to very slow accumulation rates, as would be expected on the tundra.

The Horseshoe lake core shows the highest variability in sedimentation rate of all the lakes. The core was extracted from a steep-sided sub-basin of the main lake (Fig. 6). The bathymetric profile is at a lower resolution than Bridge and Danny's lakes so it is not possible to determine exactly how the sediments drape over the bedrock. What is recognizable is that the sub-basin is only connected to the main basin by a shallow (0.5 m deep) passage. The sub-basin therefore would receive little direct sediment input from snowmelt tributaries.

### 6.2. Temporal variability in accumulation rates

It is clear that the lakes in this region respond similarly during certain time periods (Fig. 4). It is also noteworthy that the density of radiocarbon dates has an influence on the observed shifts in accumulation rate. For example, Danny's Lake and Horseshoe Lake are well-dated cores (25 and 10 radiocarbon dates, respectively) and the accumulation profiles are much more dynamic than most of the others. This is an important point because it emphasizes that

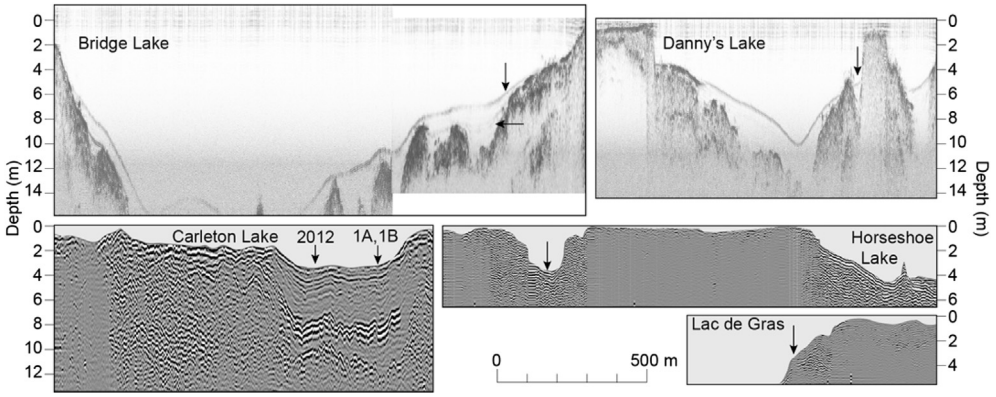


**Fig. 6.** Bathymetry profiles from six lakes with arrows showing coring sites. The horizontal arrow at Bridge Lake is pointing to a weak second reflector that is likely a result of a change in sediment deposition from clay to gyttja, as observed in the core. The coring site for Horseshoe Lake is in a sub-basin that is hydrologically connected to the main basin through a meandering path as is shown in Fig. 3.

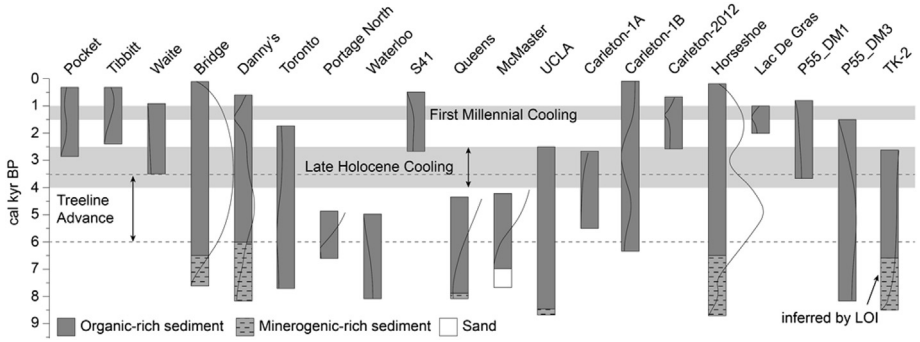


**Fig. 7.** Stratigraphic core logs plotted against cal BP. The top of each core is defined by the uppermost non-outlying radiocarbon date. Curved lines are accumulation profiles from Fig. 4b and are to be interpreted left to right is faster to slower. Time ranges for the treeline advance and Late Holocene Cooling follow Kaufman et al. (2004), and First Millennial Cooling follows Reyes et al. (2006), Hu et al. (2001), Clegg et al. (2010), and Thomas et al. (2011).

the first means of improving an age-depth model should always be to add more radiocarbon dates. However, because radiocarbon dates are expensive, it can be helpful to have an idea of when major shifts in accumulation rate for a region are to be expected. That way, a more targeted approach can be employed when refining an age-depth model using additional chronological control. Moreover, having an idea of how the accumulation rate may shift over time for an age-depth model can assist with identification of outliers as shown in section 3.3. Prior to a radiocarbon analysis, major shifts in accumulation rate can be determined either visually (changes in sediment composition) or by relatively inexpensive methods such as loss on ignition, magnetic susceptibility, or palynology.

Seven of the ten cores that extend past about 7000 cal BP show rapid accumulation rates (DT ~50 yr/cm) at the base of their record and for nearly all these sites this is an above average accumulation rate (Fig. 4). This rapid accumulation rate then steadily decreases until c. 5000 cal BP when most lakes with well-constrained age-depth models display the slowest accumulation rates. At all seven sites, this occurs just after a transition from minerogenic-rich sediment at the bottom to organic-rich sediment at the top (Fig. 7). This is a common phenomenon in paraglacial environments when sediment availability following glaciation is relatively high as long due to the presence of unstable drift material in fluvial pathways (e.g. Church and Ryder, 1972; Ballantyne, 2002). Sediment availability decreases as it is deposited, but also erosion rates are tempered as vegetation is established (Huang et al., 2004). Results from an exponential exhaustion model by Ballantyne (2002) support a decreasing accumulation rate over time as unstable sediment is deposited. Briner et al. (2010) attribute the transition from minerogenic-rich to organic-rich sediments to be indicative of the catchment for a proglacial lake getting cut off from a nearby glacier. This is to be expected as the hiatus is handled slightly differently between the two programs and it causes a major disturbance in the model. C/N ratios from Horseshoe Lake suggest that the sub-basin of Horseshoe Lake has undergone fluctuations in water depth (Griffith, 2013). Therefore, it is possible that there is a hiatus in deposition between c. 6000 and c. 4000 cal BP. A hiatus would also explain the anomalously slow accumulation rates around this period as shown in Fig. 4. While most cores show a gradual color change toward the basal sediments, the bottom 1 cm of Bridge Lake is composed of light gray clay that was likely deposited in just such a proglacial setting. We also see evidence for this shift in sediment type at Bridge Lake when looking at the bathymetry profile (Fig. 6), which shows a weak, second reflector near the bottom of the core site. Around the transition from minerogenic-rich sediments to organic-rich sediments, most lakes are characterized by slowest accumulation rates, coeval with a period of treeline advance in the region (Kaufman et al., 2004 and references therein). Similar relationships were noted for a lake in the Cathedral Mountains of British Columbia (Evans and Slaymaker, 2004) and in a crater lake in equatorial East Africa (Blaauw et al., 2011), whereby vegetation cover is thought to slow terrestrial erosion and allochthonous sediment supply to lakes due to physical stabilization of surficial materials. Following treeline advance, the accumulation rates in cores with the highest dating resolution (Danny's, Carleton-1B, and Horseshoe lakes) begin to increase again during late Holocene Cooling.

The accumulation rates for the cores from Lac de Gras, Carleton-2012 Lake, and Danny's Lake increase sharply between 1500 cal BP and 1300 cal BP, creating a small dip toward increased accumulation rates (Figs. 4 and 7). Anderson et al. (2012) also found an increase in mineral accumulation rates at inland and coastal sites from c. 1200 to 1000 cal BP on southwest Greenland. They attribute this shift to regional cooling, increased aridity, and increased delivery of allochthonous material to the lake. At Carleton Lake, a cooling event between c, 1690 and c. 940 cal BP is inferred based on

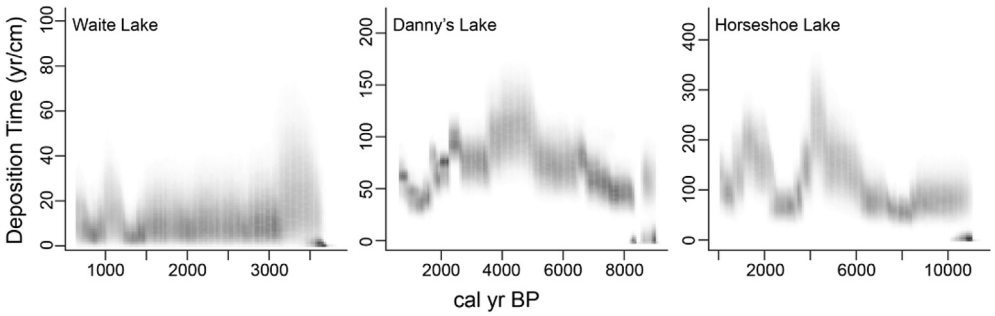


**Fig. 8.** Accumulation profiles plotted with Bacon v2.2. The darker the gray, the greater the certainty.

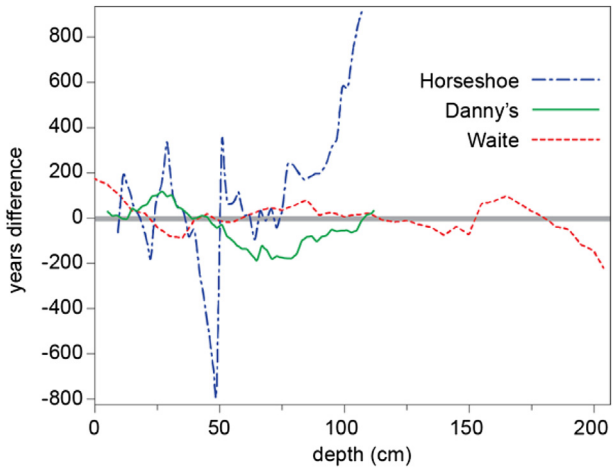


**Fig. 9.** Plot showing the difference (in years) vs. depth between the models constructed in Clam and Bacon for the Horseshoe, Danny's and Waite Lake cores.

chironomid proxy data (Upiter et al., 2014) and is temporally correlative with the timing of First Millennial Cooling, a period of cool climatic conditions in the Northern Hemisphere and documented in records from British Columbia (Reyes et al., 2006), Alaska (Hu et al., 2001; Reyes et al., 2006; Clegg et al., 2010), and the Canadian Arctic Archipelago (Thomas et al., 2011). Increased accumulation rates between c. 1500 and c. 1300 cal BP may therefore correspond to cooling in the central NWT that would have resulted in a brief period of reduced vegetation and consequently, increased erosion.

### 6.3. Accumulation rate (DT) prior

In Section 6.1 and 6.2, accumulation rates are discussed in terms of the natural environment, which is a critical first step in any modeling study. In this section, we switch gears to discuss the practical application of accumulation rates as prior information for age-depth modeling with Bayesian statistics.

The default DT prior for Bacon version 2.2 is 20 yr/cm based on the estimate from the great lakes region by Goring et al. (2012). Bacon version 2.2 is programmed to suggest an alternative DT based on round values (e.g. 10, 50, 100 yr/cm) if the default of 20 yr/cm is inappropriate for the core. As was shown for Waite Lake, 20 yr/cm is an appropriate estimate for most lakes found in the boreal forest zone, but lakes north of the treeline accumulated at much slower rates. Here we use estimates from a summary of accumulation rate data for the region to construct the age-depth models in section 5. The most striking feature of these age-depth models is how variable the accumulation rate appears to be. Fig. 8 (constructed using the *plot.acc.rate()* function in Bacon 2.2) shows a more detailed version of accumulation rate patterns for the three cores from Section 5. Waite Lake only covers the past c. 3500 years so variability is minimal, but both the longer Danny's and Horseshoe Lake records display highly variable accumulation rates (as discussed in Section 6.2). The estimates for accumulation rate entered *a priori* into the model therefore act as a guide for the age-depth model, but do not control the model entirely.

When an age-depth model is well dated, the dates themselves should guide the accumulation rate. In sections of the core with low dating resolution or age reversals, the Bayesian model can aid by incorporating prior information (Christen, 1994; Buck et al., 1996; Buck and Millard, 2004; Blaauw and Heegaard, 2012). Here we compare the Bayesian models to the Clam models in order to evaluate the effect of incorporating prior information. Because the Clam models were initially constructed with IntCal09, we reconstructed the models with IntCal13 order to ensure consistency (Supplementary Fig. 1). Moreover, a hiatus was added at 45 cm to the Horseshoe Lake model constructed with Clam. Differences between the maximum probability age of the Bayesian model and non-Bayesian model for Waite Lake, Danny's Lake, and Horseshoe Lake are presented in Fig. 9.

Waite Lake has the simplest chronology, with only one distinguishable shift in accumulation rate just before c. 1500 cal BP. The difference between the Bayesian and non-Bayesian models is 90 years at the most, which is minimal. For Danny's Lake, the difference between the two models is also fairly minimal (175 years at the most), which happens near the bottom of the model where the greatest uncertainty lies.

The difference between Bayesian and non-Bayesian age depth models for the Horseshoe Lake record does not tend to exceed 200 years, except in the region of the hiatus between c. 6000 and c. 4000 cal BP (45 cm), where the difference is nearly 800 years.

Although not shown in Fig. 9, the age-depth models constructed with Bacon have wider and more realistic calculated error ranges than for the smooth spline models constructed with Clam.

## 7. Conclusions

High resolution sampling and detailed age dating of subarctic lake cores from the Northwest Territories have provided new information about the spatial and temporal variability in lake accumulation rates in this cold, high latitude region. Based on a dataset comprised of 105 radiocarbon dates (64 new and 41 previously published) from 22 sites distributed amongst 18 lakes, we make the following conclusions:

(1) "Rapid" accumulation rates (DT ~20 yr/m) tend to occur in lakes with high productivity (boreal forest zone) or high sediment availability. Sites north of the treeline are characterized by moderate (DT ~70 yr/cm) to slow (DT > 100 yr/cm) accumulation rates with high spatial and temporal variability.

(2) Temporal shifts in accumulation rates coincide with centennial to millennial-scale climate change and the waxing and waning of vegetation cover, which is an important mechanism controlling erosion of material into lakes. Accumulation rates prior to about 7000 cal BP were rapid, reflecting recently deglaciated conditions characterized by high sediment availability and low vegetation cover. As vegetation became better established during the treeline advance, we observed a shift from minerogenic-rich to organic-rich sediments and a decrease in accumulation rates between 7000 and 4000 cal BP. This was followed by a cool period and increasing accumulation rates between 4000 cal BP and 2500 cal BP.

(3) Deposition time estimates from this research will be useful as a starting point for building robust age-depth models using Bayesian statistics and state-of-the-art software such as Bacon. Moreover, by elucidating the timing of regional shifts in accumulation rate for the Canadian Subarctic, future radiocarbon dating sampling strategies will be better informed about where to add additional radiocarbon dates to an age-depth model.

## Acknowledgments

Funding for this collaborative research project was provided by a Natural Sciences and Engineering Research Council of Canada

(NSERC) Strategic Project Grant and Discovery Grant to RTP and an Ontario Graduate Scholarship to CC. Direct and in-kind funding was provided by the Northwest Territories Geoscience Office, Polar Continental Shelf Project, the Department of Aboriginal Affairs and Northern Development Canada (by, in part, a Cumulative Impacts and Monitoring Program award to JMG), the Geological Survey of Canada, the Tibbitt to Contwoyto Winter Road Joint Venture (Erik Madsen and the crew of the Dome, Lockhart, and Lac de Gras maintenance camps), EBA Engineering Consultants Ltd., the North Slave Métis Alliance, IMG Golder, Inuvik, and Golder Associates, Yellowknife.

## Appendix A. Supplementary data

Supplementary data related to this article can be found at http://dx.doi.org/10.1016/j.quageo.2015.02.001.

## References

Anderson, N.J., Liversidge, A.C., McGowan, S., Jones, M.D., 2012. Lake and catchment response to Holocene environmental change: spatial variability along a climate gradient in southwest Greenland. J. Paleolimnol. 48, 209–222. http://dx.doi.org/10.1007/s10933-012-9616-3.

Ballantyne, C.K., 2002. Paraglacial geomorphology. Quat. Sci. Rev. 21, 1935–2017. http://dx.doi.org/10.1016/S0277-3791(02)00005-7.

Blaauw, M., 2010. Methods and code for 'classical' age-modeling of radiocarbon sequences. Quat. Geochronol. 5, 512–518. http://dx.doi.org/10.1016/j.quageo.2010.01.002.

Blaauw, M., Christen, J.A., 2005. Radiocarbon peat chronologies and environmental change. Appl. Stat. 54, 805–816. http://dx.doi.org/10.1111/j.1467-9876.2005.00516.x.

Blaauw, M., Christen, J.A., 2011. Flexible paleoclimate age-depth models using an autoregressive gamma process. Bayesian Anal. 6, 457–474. http://dx.doi.org/10.1214/ba/1339616472.

Blaauw, M., Christen, J.A., 2013. Bacon Manual – v2.2, p. 11 at: http://www.chrono.qub.ac.uk/blaauw/bacon.html (last accessed 28.02.14).

Blaauw, M., van Geel, B., Kristen, I., Plessen, B., Lyaruu, A., Engstrom, D.R., van der Plicht, J., Verschuren, D., 2011. High-resolution 14C dating of a 25,000-year lake-sediment record from equatorial East Africa. Quat. Sci. Rev. 30, 3043–3059. http://dx.doi.org/10.1016/j.quascirev.2011.07.014.

Blaauw, M., Heegaard, E., 2012. Estimation of age-depth relationships. In: Birks, H.J.B., Lotter, A.F., Juggins, S., Smol, P. (Eds.), Tracking Environmental Change Using Lake Sediments, Data Handling and Numerical Techniques, vol. 5. Springer, Netherlands, pp. 379–413. http://dx.doi.org/10.1007/978-94-007-2745-8_12.

Blass, A., Bigler, C., Grosjean, M., Sturm, M., 2007. Decadal-scale autumn temperature reconstruction back to AD 1580 inferred from the varved sediments of Lake Silvaplana (southeastern Swiss Alps). Quat. Res. 68, 184–195. http://dx.doi.org/10.1016/j.yqres.2007.05.004.

Bleeker, W., 2002. Archaean tectonics: a review, with illustrations from the Slave craton. Geol. Soc. Lond. 199, 151–181. http://dx.doi.org/10.1144/GSL.SP.2002.199.01.09. Special Publications.

Blockley, S.P.E., Blaauw, M., Bronk Ramsey, C., van der Plicht, J., 2007. Building and testing age models for radiocarbon dates in Lateglacial and Early Holocene sediments. Quat. Sci. Rev. 26, 1915–1926. http://dx.doi.org/10.1016/j.quascirev.2007.06.007.

Briner, J.P., Stewart, H.A.M., Young, N.E., Philipps, W., Losee, S., 2010. Using proglacial-threshold lakes to constrain fluctuations of the Jakobshavn Isbræ ice margin, western Greenland, during the Holocene. Quat. Sci. Rev. 29, 3861–3874. http://dx.doi.org/10.1016/j.quascirev.2010.09.005.

Bronk Ramsey, C., 2009a. Dealing with outliers and offsets in radiocarbon dating. Radiocarbon 51, 1023–1045.

Bronk Ramsey, C., 2009b. Bayesian analysis of radiocarbon dates. Radiocarbon 51, 337–360.

Buck, C.E., Cavanagh, W.G., Litton, C.D., 1996. Bayesian Approach to Interpreting Archaeological Date. Wiley, Chichester.

Buck, C.E., Millard, A.R. (Eds.), 2004. Tools for Constructing Chronologies: Crossing Disciplinary Boundaries. Springer-Verlag, London. http://dx.doi.org/10.1007/978-1-4471-0231-1.

Charman, D.J., Beilman, D.W., Blaauw, M., Booth, R.K., Brewer, S., Chambers, F.M., Christen, J.A., Gallego-Sala, A., Harrison, S.P., Hughes, P.D.M., Jackson, S.T., Korhola, A., Mauquoy, D., Mitchell, F.J.G., Prentice, I.C., van der Linden, M., De Vleeschouwer, F., Yu, Z.C., Alm, J., Bauer, I.E., Corish, Y.M.C., Garneau, M., Hohl, V., Huang, Y., Karofeld, E., Le Roux, G., Loisel, J., Moschen, R., Nichols, J.E., Nieminen, T.M., MacDonald, G.M., Phadtare, N.R., Rausch, N., Sillasoo, Ü., Swindles, G.T., Tuittila, E.-S., Ukonmaanaho, L., Välliranta, M., van Bellen, S., van Geel, B., Vitt, D.H., Zhao, Y., 2013. Climate-related changes in peatland carbon accumulation during the last millennium. Biogeosciences 10, 929–944. www.biogeosciences.net/10/929/2013/.

Christen, J.A., 1994. Bayesian Interpretation of Radiocarbon Results (Ph.D. thesis). University of Nottingham.

Christen, J.A., Pérez, E.S., 2009. A new robust statistical model for radiocarbon data. Radiocarbon 51, 1047–1059.

Church, M., Ryder, J.M., 1972. Paraglacial sedimentation: a consideration of fluvial processes conditioned by glaciation. Geol. Soc. Am. Bull. 83, 3059–3072. http://dx.doi.org/10.1130/0016-7606(1972)83[3059:PSACOF]2.0.CO;2.

Clayton, J.S., Ehrlich, W., Cann, D.B., Day, J.H., Marshall, I.B., 1977. Soils of Canada. In: Soil Inventory Research Branch, Canada, vol. II. Department of Agriculture, Ottawa, p. 239.

Clegg, B.F., Clarke, G.H., Chipman, M.L., Chou, M., Walker, I.R., Tinner, W., Hu, F.S., 2010. Six millennia of summer temperature variation based on midge analysis of lake sediments from Alaska. Quat. Sci. Rev. 29, 3308–3316. http://dx.doi.org/10.1016/j.quascirev.2010.08.001.

Dyke, A.S., Prest, V.K., 1987. Late Wisconsinan and Holocene history of the laurentide ice sheet. Géogr. Phys. Quat. 41, 237–263. http://dx.doi.org/10.7202/032681ar.

Dyke, A.S., Moore, A., Robertson, L., 2003. Deglaciation of North America. Geological Survey of Canada Open File, 1574. http://dx.doi.org/10.4095/214399.

Evans, M., Slaymaker, O., 2004. Spatial and temporal variability of sediment delivery from alpine lake basins, Cathedral Provincial Park, southern British Columbia. Geomorphology 61, 209–224. http://dx.doi.org/10.1016/j.geomorph.2003.12.007.

Edwards, T.W.D., Wolfe, B.B., MacDonald, G.M., 1996. Influence of Changing Atmospheric Circulation on Precipitation d$^{18}$O–Temperature Relations in Canada during the Holocene.

Galloway, J.M., Macumber, A.L., Patterson, R.T., Falck, H., Hadlari, T., Madsen, E., 2010. Paleoclimatological Assessment of the Southern Northwest Territories and Implicatons for the Long-term Viability of the Tibbitt to Contwoyto Winter Road, Part 1: Core Collection. Northwest Territories Geoscience Office, p. 21. NWT Open Report 2010-002.

Glew, J.R., 1991. Miniature gravity corer for recovering short sediment cores. J. Paleolimnol. 5, 285–287. http://dx.doi.org/10.1007/BF00200351.

Glew, J.R., Smol, J.P., Last, W.M., 2001. Sediment core collection and extrusion. In: Last, W.M., Smol, J.P. (Eds.), Tracking Environmental Changes Using Lake Sediments, Basin analysis, Coring and Chronological Techniques, vol. 1. Kluwer Academic Publishers, Dordrecht, pp. 73–105.

Goring, S., Williams, J.W., Blois, J.L., Jackson, S.T., Paciorek, C.J., Booth, R.K., Marlon, J.R., Blaauw, M., Christen, J.A., 2012. Accumulation rates in the northeastern United States during the Holocene: establishing valid priors for Bayesian age models. Quat. Sci. Rev. 48, 54–60. http://dx.doi.org/10.1016/j.quascirev.2012.05.019.

Griffith, F., 2013. Holocene and Recent Paleoclimate Investigations Using Carbon and Nitrogen Isotopes from Bulk Sediment of two Subarctic Lakes, Central Northwest Territories. University of Ottawa (MSc thesis).

Helmstaedt, H., 2009. Crust-mantle coupling revisited: the archean slave craton, NWT, Canada. Lithos 112S, 1055–1068. http://dx.doi.org/10.1016/j.lithos.2009.04.046.

Hu, F.S., Ito, E., Brown, T.A., Curry, B.B., Engstrom, D.R., 2001. Pronounced climatic variations in Alaska during the last two millennia. Proc. Natl. Acad. Sci. 98, 10552–10556. http://dx.doi.org/10.1073/pnas.181333798.

Hua, Q., Barbetti, M., 2004. Review of tropospheric bomb 14C data for carbon cycle modeling and age calibration purposes. Radiocarbon 46, 1273–1298.

Hua, Q., Barbetti, M., Rakowski, A.Z., 2013. Atmospheric radiocarbon for the period 1950-2010. Radiocarbon 55. http://dx.doi.org/10.2458/azu_js_rc.v55i2.16177.

Huang, C.C., MacDonald, G., Cwynar, L., 2004. Holocene landscape development and climatic change in the low arctic, Northwest Territories, Canada. Palaeogeogr. Palaeoclimatol. Palaeoecol. 205, 221–234. http://dx.doi.org/10.1016/j.palaeo.2003.12.009.

Karst-Riddoch, T., Pisaric, M., Smol, J., 2005. Diatom responses to 20th century climate-related environmental changes in high-elevation mountain lakes of the northern Canadian Cordillera. J. Paleolimnol. 33, 265–282.

Kaufman, D.S., Ager, T.A., Anderson, N.J., Anderson, P.M., Andrews, J.T., Bartlein, P.J., Brubaker, L.B., Coats, L.L., Cwynar, L.C., Duvall, M.L., Dyke, A.S., Edwards, M.E., Eisner, W.R., Gajewski, K., Geirsdóttir, A., Hu, F.S., Jennings, A.E., Kaplan, M.R., Kerwin, M.W., Lozhkin, A.V., MacDonald, G.M., Miller, G.H., Mock, C.J., Oswald, W.W., Otto-Bliesner, B.L., Porinchu, D.F., Rühland, K., Smol, J.P., Steig, E.J., Wolfe, B.B., 2004. Holocene thermal maximum in the western Arctic (0–180 W). Quat. Sci. Rev. 23, 529–560. http://dx.doi.org/10.1016/j.quascirev.2003.09.007.

Koff, T., Punninga, J.-M., Kangura, M., 2000. Impact of forest disturbance on the pollen influx in lake sediments during the last century. Rev. Palaeobot. Palynol. 111, 19–29. http://dx.doi.org/10.1016/S0034-6667(00)00013-0.

Kulbe, T., Niederreiter Jr., R., 2003. Freeze coring of soft surface sediments at a water depth of several hundred meters. J. Paleolimnol. 29, 257–263. http://dx.doi.org/10.1023/A:1023209632092.

Lehman, J., 1975. Reconstructing the rate of accumulation of lake sediment: the effect of sediment focusing. Quat. Res. 5, 541–550. http://dx.doi.org/10.1016/0033-5894(75)90015-0.

Lotter, A.F., Renberg, I., Hansson, H., Stöckli, R., Sturm, M., 1997. A remote controlled freeze corer for sampling unconsolidated surface sediments. Aquat. Sci. 59, 295–303.

MacDonald, G.M., Edwards, T.W.D., Moser, K.A., Pienitz, R., Smol, J.P., 1993. Rapid response of treeline vegetation and lakes to past climate warming. Nature 361, 243–246. http://dx.doi.org/10.1038/361243a0.

MacDonald, G.M., Porinchu, D.F., Rolland, N., Kremenetsky, K.V., Kaufman, D.S., 2009. Paleolimnological evidence of the response of the central Canadian treeline zone to radiative forcing and hemispheric patterns of temperature change over the past 2000 years. J. Paleolimnol. 41, 129–141. http://dx.doi.org/10.1007/s10933-008-9250-2.

Macumber, A.L., Patterson, R.T., Neville, L.A., Falck, H., 2011. A sledge microtome for high resolution subsampling of freeze cores. J. Paleolimnol. 45, 307–310. http://dx.doi.org/10.1007/s10933-010-9487-4.

Macumber, A.L., Neville, L.A., Galloway, J.M., Patterson, R.T., Falck, H., Swindles, G., Crann, C., Clark, I., Gammon, P., Madsen, E., 2012. Paleoclimatological Assessment of the Northwest Territories and Implications for the Long-term Viability of the Tibbitt to Contwoyto Winter Road, Part II: March 2010 Field Season Results. Northwest Territories Geoscience Office, p. 83. NWT Open Report 2011-010.

Marlon, J., Bartlein, P.J., Whitlock, C., 2006. Fire-fuel-climate linkages in the northwestern USA during the Holocene. Holocene 16, 1059–1071. http://dx.doi.org/10.1177/0959683606069396.

Miller, G., Brigham-Grette, J., Alley, R., Anderson, L., Bauch, H., Douglas, M., Edwards, M., Elias, S., Finney, B., Fitzpatrick, J., Funder, S., Herbert, T., Hinzman, L., Kaufman, D.S., MacDonald, G.M., Polyak, L., Robock, A., Serreze, M., Smol, J., Spielhagen, R., White, J., Wolfe, A., Wolff, E., 2010. Temperature and precipitation history of the Arctic. Quat. Sci. Rev. 29, 1679–1715.

Moser, K.A., MacDonald, G.M., 1990. Holocene vegetation change at treeline north of Yellowknife, Northwest Territories, Canada. Quat. Res. 34, 227–239. http://dx.doi.org/10.1016/0033-5894(90)90033-H.

Padgham, W.A., Fyson, W.K., 1992. The slave province: a distinct Archean craton. Can. J. Earth Sci. 29, 2072–2086. http://dx.doi.org/10.1139/e92-165.

Paul, C.A., Rühland, K.M., Smol, J.P., 2010. Diatom-inferred climatic and environmental changes over the last ~9000 years from a low Arctic (Nunavut, Canada) tundra lake. Palaeogeogr. Palaeoclimatol. Palaeoecol. 291, 205–216.

Pienitz, R., Smol, J.P., MacDonald, G.M., 1999. Paleolimnological reconstruction of Holocene climate trends from two boreal treeline lakes, Northwest Territories, Canada. Arct. Antarct. Alp. Res. 31, 82–93. http://dx.doi.org/10.2307/1552625.

Punning, J.-M., Koff, T., Sakson, M., Kangur, M., 2007a. Holocene pattern of organic carbon accumulation in a small lake in Estonia. Pol. J. Ecol. 55, 5–14.

Punning, J.-M., Boyle, J.F., Terasmaa, J., Vaasma, T., Mikomägi, A., 2007b. Changes in lake sediment structure and composition caused by human impact: repeated studies of Lake Martiska, Estonia. Holocene 17, 145–151. http://dx.doi.org/10.1177/0959683607073297.

Rampton, V.N., 2000. Large-scale effects of subglacial meltwater flow in the southern Slave Province, Northwest Territories, Canada. Can. J. Earth Sci. 37, 81–93. http://dx.doi.org/10.1139/e99-110.

Reimer, P.J., Brown, T.J., Reimer, R.W., 2004. Discussion: reporting and calibration of post-bomb 14C data. Radiocarbon 46, 1299–1304.

Reimer, P.J., Baillie, M.G.L., Bard, E., Bayliss, A., Beck, J.W., Blackwell, P.G., Bronk Ramsey, C., Buck, C.E., Burr, G.S., Edwards, R.L., Friedrich, M., Grootes, P.M., Guilderson, T.P., Hajdas, I., Heaton, T.J., Hogg, A.G., Hughen, K.A., Kaiser, K.F., Kromer, B., McCormac, F.G., Manning, S.W., Reimer, R.W., Richards, D.A., Southon, J.R., Talamo, S., Turney, C.S.M., van der Plicht, J., Weyhenmeyer, C.E., 2009. IntCal09 and Marine09 radiocarbon age calibration curves, 0-50,000 years cal BP. Radiocarbon 51, 1111–1150.

Reimer, P.J., Bard, E., Bayliss, A., Beck, J.W., Blackwell, P.G., Bronk Ramsey, C., Buck, C.E., Cheng, H., Edwards, R.L., Friedrich, M., Grootes, P.M., Guilderson, T.P., Haflidason, H., Hajdas, I., Hatté, C., Heaton, T.J., Hoffmann, D.L., Hogg, A.G., Hughen, K.A., Kaiser, K.F., Kromer, B., Manning, S.W., Niu, M., Reimer, R.W., Richards, D.A., Scott, E.M., Southon, J.R., Staff, R.A., Turney, C.S.M., van der Plicht, J., 2013. IntCal13 and Marine13 radiocarbon age calibration curves 0–50,000 years cal BP. Radiocarbon 55, 1869–1887. http://dx.doi.org/10.2458/azu_js_rc.55.16947.

Reyes, A.V., Wiles, G.C., Smith, D.J., Barclay, D.J., Allen, S., Jackson, S., Larocque, S., Laxton, S., Lewis, D., Calkin, P.E., Clague, J.J., 2006. Expansion of alpine glaciers in Pacific North America in the first millennium A.D. Geology 34, 57–60. http://dx.doi.org/10.1130/G21902.1.

Rühland, K., Smol, J.P., 2005. Diatom shifts as evidence for recent Subarctic warming in a remote tundra lake, NWT, Canada. Palaeogeogr. Palaeoclimatol. Palaeoecol. 226, 1–16. http://dx.doi.org/10.1016/j.palaeo.2005.05.001.

Saulnier-Talbot, E., Pienitz, R., Stafford Jr., T.W., 2009. Establishing Holocene sediment core chronologies for northern Ungava lakes, Canada, using humic acids (AMS 14C) and 210Pb. Quat. Geochronol. 4, 278–287. http://dx.doi.org/10.1016/j.quageo.2009.02.018.

Smith, D.G., 1994. Glacial Lake McConnell: paleogeography, age, duration, and associated river deltas, Mackenzie River Basin, Western Canada. Quat. Sci. Rev. 13, 829–843. http://dx.doi.org/10.1016/0277-3791(94)90004-3.

Sulphur, et al., 2015. Holocene Vegetation and Fire Regime Changes in Central Northwest Territories: Palynological Analyses of Danny's and Waite lakes (in preparation).

Stuiver, M., Reimer, P.J., 1993. Extended 14C database and revised Calib 3.0 14C age calibration program. Radiocarbon 35, 215–230.

Terasmaa, J., 2011. Lake basin development in the Holocene and its impact on the sedimentation dynamics in a small lake (southern Estonia). Est. J. Earth Sci. 60 (3), 159–171. http://dx.doi.org/10.3176/earth.2011.3.04.

Thomas, E.K., Briner, J.P., Axford, Y., Francis, D.R., Miller, G.H., Walker, I.R., 2011. A 2000-yr-long multi-proxy lacustrine record from central Baffin Island, Arctic Canada reveals first millennium AD cold period. Quat. Res. 75, 491–500. http://dx.doi.org/10.1016/j.yqres.2011.03.003.

Upiter, L.M., Vermaire, J.C., Patterson, R.T., Crann, C., Galloway, J.M., Macumber, A.L., Neville, L.A., Swindles, G.T., Falck, H., Roe, H.M., Pisaric, M.F.J., 2014. A mid- to late Holocene chironomid-inferred temperature reconstruction for the central Northwest territories, Canada. J. Paleolimnol. 52, 11–26. http://dx.doi.org/10.1007/s10933-014-9775-5.

Webb, R.S., Webb, T., 1988. Rates of sediment accumulation in pollen cores from small lakes and mires of eastern North America. Quat. Res. 30, 284–297. http://dx.doi.org/10.1016/0033-5894(88)90004-X.

Wedel, J.H., Smart, A., Squires, P., 1990. An Overview Study of the Yellowknife River Basin, N.W.T. N.W.T. Programs: Inland Waters Directorate Conservation and Protection. Western and Northern Region, Environment Canada, Ottawa.

Wolfe, B.B., Edwards, T.W.D., Aravena, R., MacDonald, G.M., 1996. Rapid Holocene hydrologic change along boreal tree-line revealed by ™13C and ™18O in organic lake sediments, Northwest Territories, Canada. J. Paleolimnol. 15, 171–181. http://dx.doi.org/10.1007/BF00196779.

Wright Jr., R.G., Mann, D.H., Glaser, P.H., 1984. Piston cores for peat and lake sediments. Ecology 65, 657–659. http://dx.doi.org/10.2307/1941430.